# Hydrogen from biomass gasification

Biomass harvesting,
Photo: Bioenergy2020+

IEA Bioenergy

IEA Bioenergy: Task 33: December 2018

# Hydrogen from biomass gasification

Matthias Binder, Michael Kraussler, Matthias Kuba, and Markus Luisser

Edited by Reinhard Rauch



ISBN, 978-1-910154-59-5

**Published by IEA Bioenergy**

# Executive Summary

Hydrogen will be an important renewable secondary energy carrier for the future. Today, hydrogen is predominantly produced from fossil fuels. Hydrogen production from biomass via gasification can be an auspicious alternative for future decarbonized applications, which are based on renewable and carbon-dioxide-neutral produced hydrogen.

This study gives an overview of possible ways to produce hydrogen via biomass gasification. First, an overview of the current market situation is given. Then, hydrogen production based on biomass gasification is explained. Two different hydrogen production routes, based on biomass gasification, were investigated in more detail. Hydrogen production was investigated for steam gasification and sorption enhanced reforming.

Both routes assessed, appear suitable for hydrogen production. Biomass to hydrogen efficiencies (LHV based) of up to 69% are achieved and a techno-economic study shows, hydrogen selling prices of down to 2.7 EUR·kg$^{-1}$ (or 79 EUR·MWh$^{-1}$).

Overall it can be stated, that governmental support and subsidies are necessary for successful implementation of hydrogen production based on biomass gasification technologies. Especially the first 15 years of the development towards market maturity and stable operation and production are critical and will need political support systems.

For evaluating the process chains it can be stated that gas upgrading unit operations, such as WGS, scrubbers and PSA units, are technologically proven and available on the market for similar applications. Furthermore, the feedstock spectrum has to be broadened in the future to increase the flexibility of the process and improve the overall economic feasibility.

# Content

# Reasons to produce renewable hydrogen

The growing global energy demand is mostly covered by fossil primary energy sources. Since the beginning of the industrialization, usages and requirements for energy carriers changed according to the state of science and technology. Over time, consumption of fuels has moved from solids such as wood and then coal, followed by a parallel use of liquid crude oil to a, nowadays, also strong increase in the use of natural gas. Disregarding the traditional use of wood, this has led to a shift from carbon to hydrogen with respect to the molar ratio of the fuels. This trend of decarbonization could be enhanced by strengthened substitution of the fossil fuels with hydrogen. (Dunn, 2002; Hefner III, 2002)

The Paris Agreement, also referred to as Paris climate accord, is an agreement within the United Nations Framework Convention on Climate Change (UNFCCC), which for the first time brought all nations into a common cause to set ambitious goals for keeping the global temperature rise below 2 °C. Despite that the United States of America have left the agreement. Nevertheless, it is the strongest international framework for the development of alternative sustainable technologies so far and promotes the application of renewable sources in industrial processes. (*Paris Agreement*, 2015)

Nowadays, hydrogen is an important intermediate in chemical industry and refineries. The annual production of hydrogen was around 100 million tonnes in 2014 (50 % captive, 44 % by-product and 6 % merchant production), or 12 EJ on an LHV basis (equivalent of some 2 % of the global primary energy consumption). Renewable hydrogen is seen as an important secondary energy carrier of the future and could be used directly as fuel and feedstock for further syntheses as well as for the generation and storage of electricity. (Ball and Wietschel, 2009; Liu et al., 2010) Today, 95% of the global hydrogen production is based on fossil fuels, which is then associated with huge carbon dioxide emissions. A small share of $H_2$ is generated by water electrolysis using electricity. As long as supplied electricity generates carbon dioxide emissions, this does not solve the dilemma of greenhouse gases with a sustainable effect, as electricity is generated using fossil fuels. Hydrogen from renewable energy sources is discussed as an alternative to solve the dilemma of greenhouse gases, especially carbon dioxide. This can be a step in the direction of a decarbonized energy system and hydrogen could play an important role in meeting the world's future demand for energy. (Balat and Kırtay, 2010) The worldwide hydrogen production is mainly used by four consumers: ammonia production 50%, refinery applications 22%, methanol production 14%, and various reduction processes 7%. The rest of 7% is spread to other consumers. The worldwide demand for hydrogen is growing, e.g. from increased production of ammonia and methanol as well as from because of the need to process heavier and dirtier feedstocks in refineries and more hydrogen for hydro-desulfurization processes is also required because of more stringent environmental regulations which claim the production of almost sulfur free products. In addition, the evolving interest in using hydrogen as an energy carrier will result in a large hydrogen demand in the future. (Düker, 2011; Liu et al., 2010) A more detailed market analysis will be presented in the next chapter. The above mentioned facts lead to the question of the nature of future hydrogen production, which is currently based on non-renewable sources.

Generally, hydrogen production processes can be classified in three categories: electrochemical, biological and thermochemical methods. All of these methods can be realized on a renewable base. In the case of electrochemical methods, electricity must then be generated by sustainable sources of energy.

The most important electrochemical method is the already mentioned electrolysis of water. Driven by electric energy, water molecules (as liquid or steam) are separated into hydrogen and oxygen. Industrial electrolyzers operate at efficiencies of 52–85%, strongly depending on the size and type of the apparatus. Water electrolysis is the key element of power-to-hydrocarbon concepts which currently attracts a lot of interest. The definition of power-to-hydrocarbon is here not limited to the production of hydrocarbons, but also includes hydrogen production. The fluctuating output of renewable electricity generated by wind power and photovoltaics creates a growing need for energy storage. As the capacity of pumped storage hydro power stations is limited, the conversion of electricity into chemical energy by means of electrolysis represents a promising complementing technology. This explains why an increasing number of power-to-gas facilities are currently being devleoped. These facilities usually employ the commercially available alkaline electrolyzers. Some sites also use proton exchange membrane (PEM) electrolyzers for the electrolysis of water. Also, other forms of electrolyzers (SOEC, MCEC) are being demonstrated. The generated hydrogen can be stored and reconverted into electricity in times of an undersupply. Few plants have also demonstrated the application of the generated hydrogen within a methanation process enabling the feeding of methane into the natural gas grid. (Gahleitner, 2013)

Hydrogen can be produced biologically or photo-biologically by different microorganisms over a series of metabolisms. The advantages of these methods are the operation at ambient pressure and temperature as well as the usage of renewable feedstock and/or solar energy. However, the state-of-the-art is at laboratory scale and the practical applications still need to be demonstrated. A series of hydrogen producing metabolic pathways can be distinguished: Biophotolysis of water using green algae or cyanobacteria, biological water gas shift reaction, photo-fermentation, dark fermentation and hybrid systems. The biological hydrogen production is catalyzed using hydrogen-producing enzymes, such as hydrogenase and nitrogenase. These enzymes employ active centers including complexes of iron, molybdenum or nickel. The same metals are also used in commercial catalyst for thermochemical hydrogen production. Cofactors usually contain sulfur. Dark fermentation and photofermentation are considered to be the most promising approaches for hydrogen production by means of microorganisms. (Chaubey et al., 2013; Ni et al., 2006) However, such methods are still at laboratory scale and cannot be expected to be industrially available for still quite some time.

Thermochemical routes, based on fossil fuels, are state of the art for industrial scale $H_2$ production. Renewable hydrogen via thermochemical methods can be achieved using biomass as the feedstock. Hydrogen production from hydrocarbons such as fossil fuels and biomass involves conversion technologies such as reforming, gasification, and pyrolysis. These processes provide a synthesis gas, mainly consisting of hydrogen and carbon monoxide. This synthesis gas can be subjected to downstream processes in order to produce pure hydrogen.

(Arregi et al., 2018) compared different routes for hydrogen production from biomass, including gasification-based processes. In the study, also hydrogen production via pyrolysis was included. Figure 1 shows an overview of the production routes for hydrogen from lignocellulosic biomass. Different concepts (fixed bed, fluidized bed, entrained flow, etc.) were investigated and compared with each other. This comprehensive review of existing research and development has identified steam gasification as one of the main thermo-chemical routes. In the development of steam gasification for hydrogen production, fluidized bed gasification is one of the major technologies in today's research and development.

The present report relates to thermal gasification only such that pyrolysis pathways will not be analyzed. Further results for hydrogen production via different steam gasification routes will be highlighted later on.

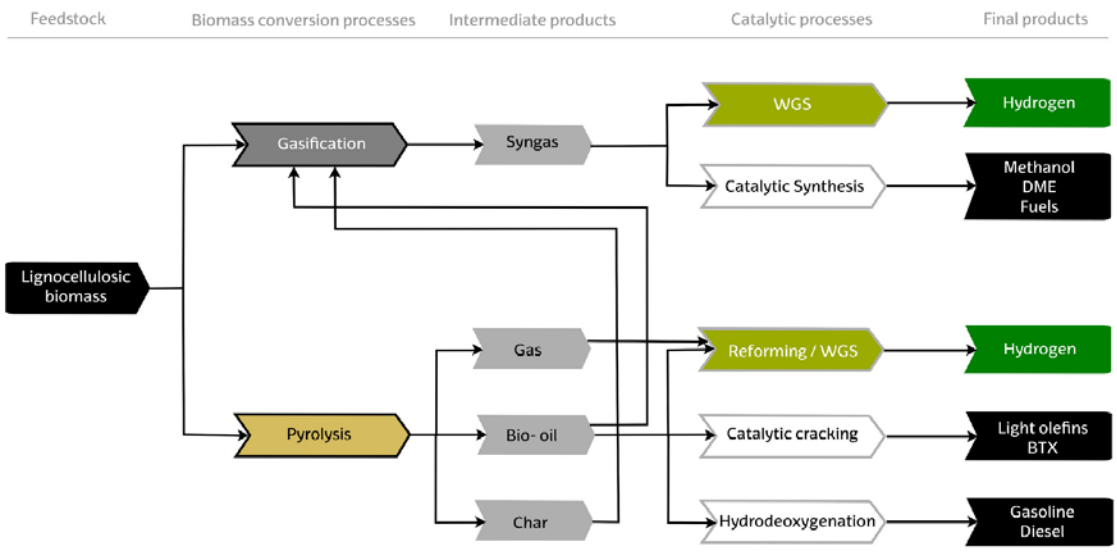


Figure 1: Schematic representation of the main processes involved in a thermochemical conversion route, based on lignocellulosic biomass. (Arregi et al., 2018)

Based on available literature in the field of biomass-gasification-based hydrogen production, the present study will focus on fluidized bed steam gasification as conversion step for biomass. There is yet no comprehensive assessment for possible production routes based on fluidized bed steam gasification for hydrogen generation available. Thus, different process chains for the production of hydrogen based on different fluidized bed steam gasification technologies will be assessed and discussed regarding their development state. Overall information on gasification and the necessary gas upgrading unit operation will establish the level of know-how to further evaluate in more detail chosen technological process chains.

# Overview about markets and applications of renewable hydrogen

This chapter will give an overview of the current situation of markets and applications of renewable $H_2$. Furthermore, an outlook regarding the development of the $H_2$ market will be given. Figure 2 shows an overview of the global $H_2$ demand in 2010 based on the captive market and a prediction of its development until 2025. The increase of about 17% will be based on the rising demand for the production of ammonia, methanol, and petroleum refinery operations.

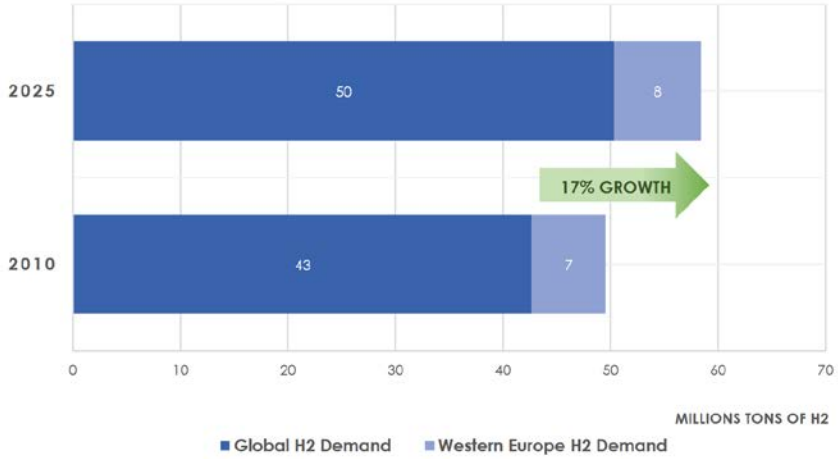


Figure 2: World Hydrogen Industry Study 2010 by Freedonia and Production and Utilization of Green Hydrogen by The Linde Group. (Fraile et al., 2015)

Figure 3 shows the current sources of hydrogen. As mentioned before, hydrogen production is nowadays dominated by fossil sources and a small share of electrolysis. The share of biomass-based hydrogen production is yet negligible in the overall production. Nevertheless, the market analysis will show its potential and the political aim to include biomass gasification-based hydrogen production into the overall strategy.

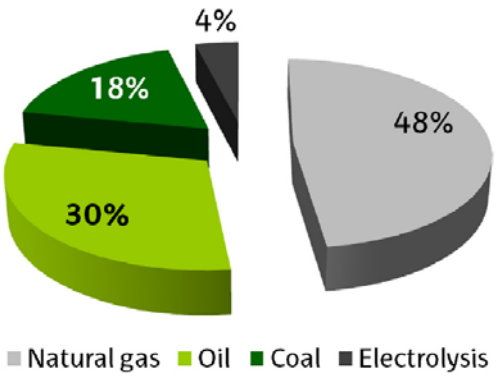


Figure 3: Current feedstock used for $H_2$ production. (Arregi et al., 2018)

In the following, the market analysis will be divided into three scales, each categorized to a field of application:

- Small scale - hydrogen filling stations: 15 to 50 $kg \cdot h^{-1}$ (0.5 MW to 1.7 MW $H_2$ capacity)
- Medium scale - hydrogen for refineries: 1 000 to 3 000 $kg \cdot h^{-1}$ (33 MW to 100 MW $H_2$ capacity)
- Large scale - hydrogen for industrial areas: 2 000 to 10 000 $kg \cdot h^{-1}$ (66 MW to 333 MW $H_2$ capacity)

For each segment, findings from available literature were reviewed and selected information relevant for this study will be presented and discussed.

## SMALL SCALE - HYDROGEN FILLING STATIONS

Fuel cell vehicles are a promising and $CO_2$-neutral alternative to conventional transportation vehicles. Such fuel cell vehicles are capable of long trips (over 500 km) and have a shorter refueling time compared to solely electric vehicles, which is comparably to conventional vehicles. However, the progress of implementing fuel cell vehicles has still barriers. On one hand, the fueling infrastructure for hydrogen is still limited and on the other hand the fuel cell vehicle production costs need to drop significantly from their current levels to reach market maturity.

Figure 4 summarizes the global fuel cell vehicle deployment since 2012. In total, about 4 500 cumulative vehicles as of July 2017 have been produced (the total passenger car fleet is approaching 1 billion cars and annually some 75 million cars are produced). It is noteworthy to mention, that fuel cell deployment in 2016 was about six times higher than in 2015. Data for 2017 was not available when this study was conducted, but the available numbers from January until July 2017 suggest another increase in production.

Also, the infrastructure of refueling stations is growing significantly according to Figure 5. For 2017, the deployment of stations and vehicles is shown for seven markets, labelled for selected countries or respectively regions. It can be seen, that California and Japan are fastest in building up a hydrogen-based infrastructure. The red points on the upper right are expected projections from national planning according to the government and industry goals. As it can be seen, the projected increase is significant compared to the current numbers.

Even though the growth of hydrogen infrastructure is evident, the future markets are still hard to foresee, as circumstances for hydrogen mobility can quickly change. In the competition of different technologies for future mobility, no clear pathway is yet determined. Electric cars have gained significant increase of political support, but are still facing challenges when it comes to range capability, fueling time, and similarly to hydrogen vehicles, are still problematic regarding the complete value chain including electricity production. Even though the share of renewable electricity is increasing significantly, changing the complete mobility sector to purely electric mobility will not be manageable in the near to medium future, as there is also a remaining life-

time of vehicles in the existing fleet and in liquid-fueled cars will still be sold in the future. Hence, from a Paris Agreement perspective, development of different solutions, energy saving, biofuels, e-mobility and fuel cells should be pursued in order to address different market needs and segments.

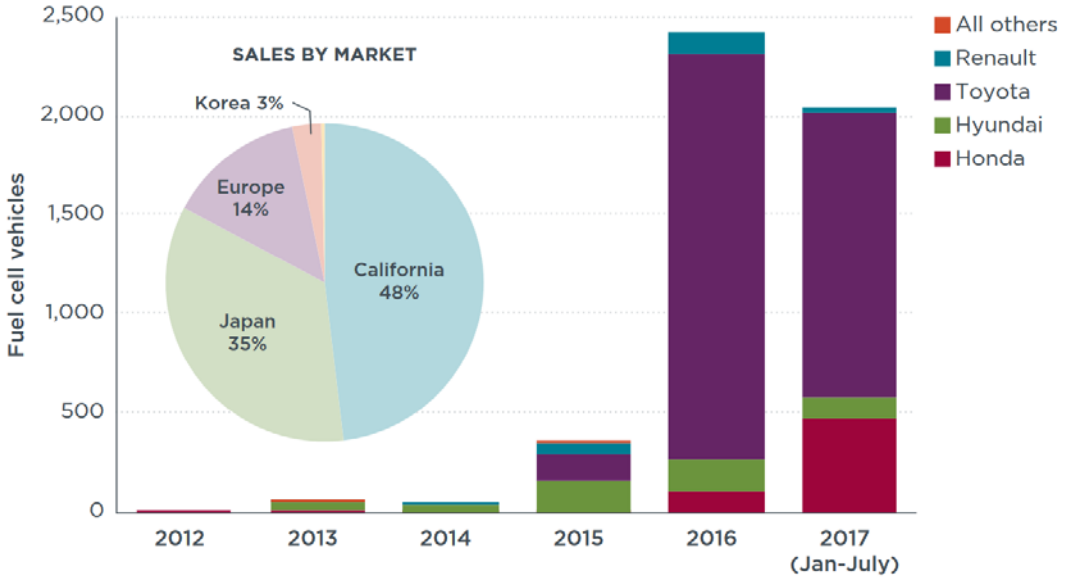


Figure 4: New fuel cell vehicle deployments for 2012 through mid-2017, by company and locale. (Insenstadt and Lutsey, 2017)

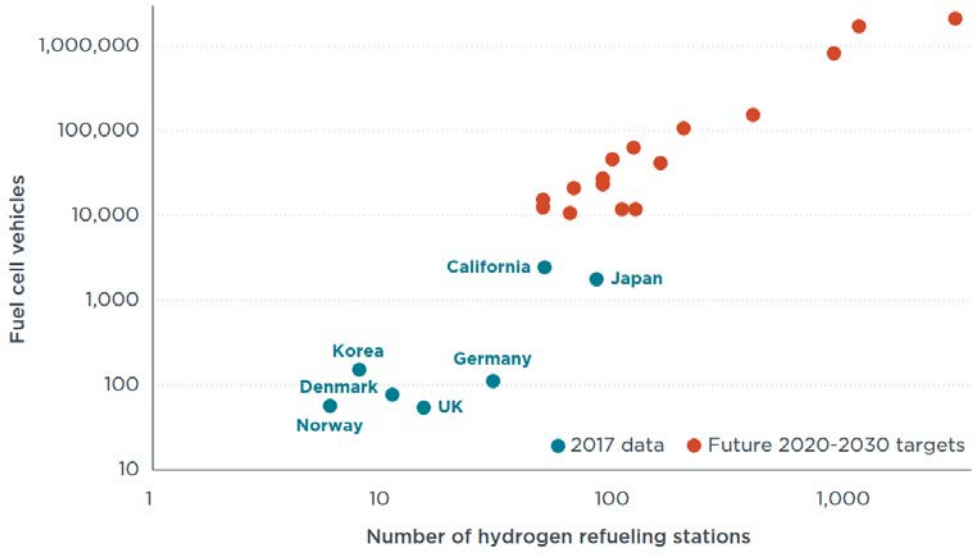


Figure 5: Summary of current hydrogen refueling station deployment, and government and industry projections and goals for initial hydrogen station and fuel cell vehicle deployment through 2025. (Insenstadt and Lutsey, 2017)

Figure 6 shows the modelled hydrogen station cost for varying hydrogen daily fueling volume. It becomes evident that larger stations – meaning larger daily hydrogen throughput – have higher

overall costs. However, they are more economically based on their cost per kilogram of hydrogen delivered. In this context another point has to be considered. Hydrogen delivery and storage strongly influences the stations' costs. Whereas gaseous hydrogen has higher component costs for compression and equipment (as high pressure cascade equipment is needed) and running costs for continuously compressing hydrogen for dispensation, liquid hydrogen has higher costs for storage, pumping and evaporation. Liquid hydrogen shows financial advantages for dispensation, compression and logistics when it comes to delivery at high daily volumes. However, this work does not take hydrogen storage and distribution into account. Data on hydrogen storage or hydrogen distribution can be found e.g. in (Zech et al., 2013).

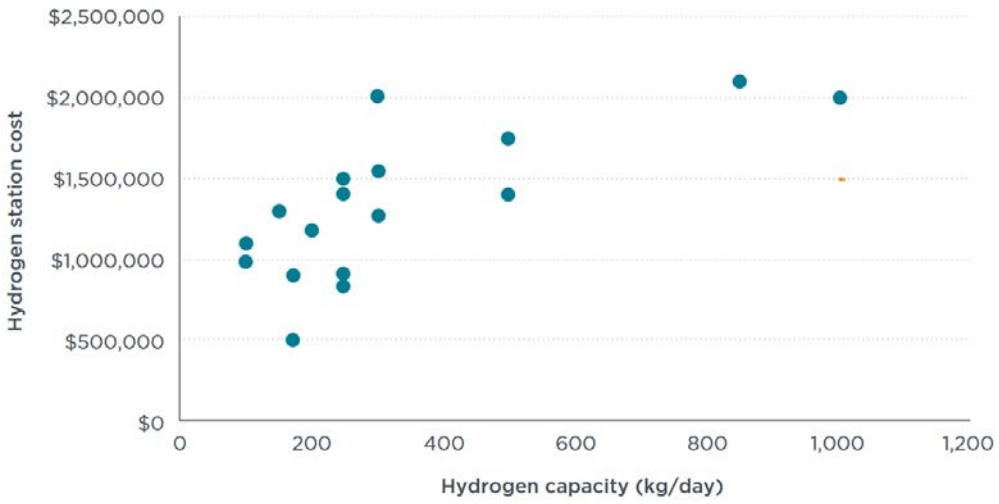


Figure 6: Modeled hydrogen station cost for varying hydrogen daily volume. (Insenstadt and Lutsey, 2017)

Figure 7 shows a comparison of different studies conducted regarding the $H_2$ demand for road transport in Europe. As it can be seen, depending on the assumed circumstances, including policy support and mobility initiatives, the projections differ significantly from each other. This shows that there is still a high uncertainty in the further market development for $H_2$. The studies compared were projecting the fuel cell electric vehicle roadmaps. A study by CertifHy from the year 2015 estimated a European $H_2$ consumption of around $7.9 \cdot 10^8$ $kg \cdot a^{-1}$. In this projection, four regions, namely France, UK, Germany and Scandinavia hold a market share of around 60%, as they have implemented the $H_2$-mobility programs early on and thus represent the strongest market players in Europe.

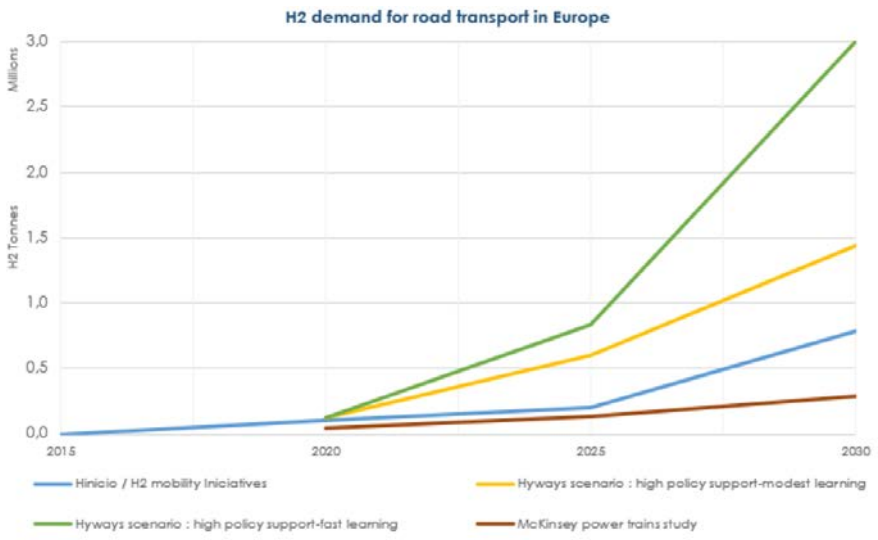


Figure 7: Comparative analysis of existing roadmaps for FCEV and $H_2$ demand for transport. (Fraile et al., 2015)

In summary, the development of $H_2$ in the mobility sector is currently limited due to unclear policy support. The production of hydrogen fuel cell vehicles as well as the fueling infrastructure is increasing; however the development of the market is still in a state of high uncertainty.

## MEDIUM SCALE - HYDROGEN FOR REFINERIES

Refineries are the typical example for medium scale usage of hydrogen and the second largest market for (renewable) hydrogen. Currently, about 30% of the market share is related to the refinery sector, with a total amount of about $2.1 \cdot 10^9$ kg·a$^{-1}$ of $H_2$ (excluding by-product hydrogen). Figure 8 shows the comparison of the market share in comparison to the chemical industry and metal processing.

Hydrogen is mainly used for hydrogenation processes, such as hydrodesulfurization, or where heavier crudes are cracked and the hydrogen ratio in the molecules is increased to produce lighter crudes. In refinery processes the purity of hydrogen needs to be high.

The consumption of hydrogen for single refinery sites can differ significantly depending on the employed refinery units. To get an estimate of the range, the consumption for different refinery sites varies from about $7.2 \cdot 10^6$ to about $1.1 \cdot 10^8$ kg·a$^{-1}$, modern large scale refineries have reported numbers up to $2.9 \cdot 10^8$ kg a$^{-1}$. (Fraile et al., 2015)

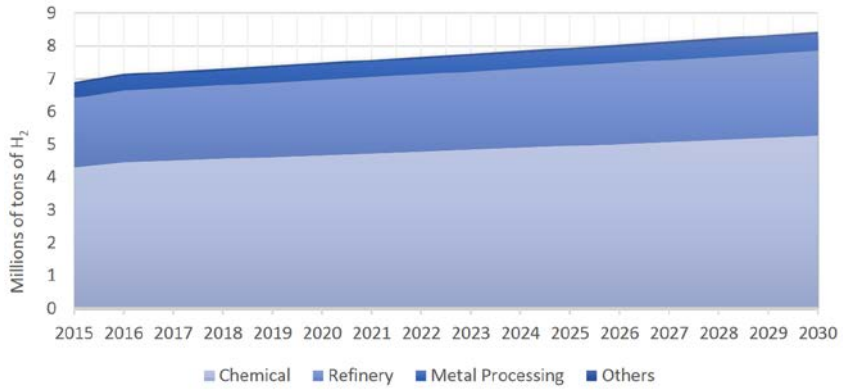


Figure 8: Industry market share, forecast. (Fraile et al., 2015)

Figure 9 shows a summary of the industry and market share of hydrogen in EU28 in 2013. Furthermore, it can be seen that both the chemical industry and refining, which together have a market share of more than 90%, are dependent on a $H_2$ supply system in the form of pipelines of large on-site $H_2$ production. The total hydrogen demand of the two largest sectors, refining and the chemical industry, is about $6.4 \cdot 10^9$ $kg \cdot a^{-1}$ and is currently almost completely based on hydrogen production from fossil fuels.

| INDUSTRY & MARKET SHARE | KEY APPLICATIONS | SUPPLY SYSTEM | H2 DEMAND |
|---|---|---|---|
| General Industry 1% | • Semiconductor<br>• Propellant Fuel<br>• Glass Production<br>• Hydrogenation of Fats<br>• Cooling of electrical Generators | • Small on-site<br>• Tube trailers<br>• Cylinders<br>• Liquid H2 | LOW<br>>0.07 Mtons |
| Metal Working 6% | • Iron Reduction<br>• Blanketing gas<br>• Forming gas | • Cylinders<br>• Tube trailers | MEDIUM<br>0.41 Mtons |
| Refining 30% | • Hydrocracking<br>• Hydrotreating | • Pipeline<br>• Large On-site | 2.1 Mtons |
| Chemical 63% | • Ammonia<br>• Methanol<br>• Polymers<br>• Resins | • Pipeline<br>• Large On-site | HIGH<br>4.3 Mtons |

Figure 9: Summary of the industry and market share of hydrogen in EU28 in 2013. (Fraile et al., 2015)

## LARGE SCALE - HYDROGEN FOR INDUSTRIAL AREAS

As mentioned above, the chemical industry represents about 63% of the total global hydrogen demand. Figure 10 shows a chart of the main segments in the chemical industry. As it can be seen, of the 63% the main share of 84% is ammonia production. Thus, ammonia production is by far the largest market for hydrogen in the presence as well as in the foreseeable future. With 12% methanol is another important sector for hydrogen consumption. The other noteworthy industry fields are polymer (nylon) production as well as resin (polyurethane, methylene-diphenyl-diisocyanate (MDI) and toluene-diisocyanate (TDI)) production, each with a share of about 2% within the chemical industry market.

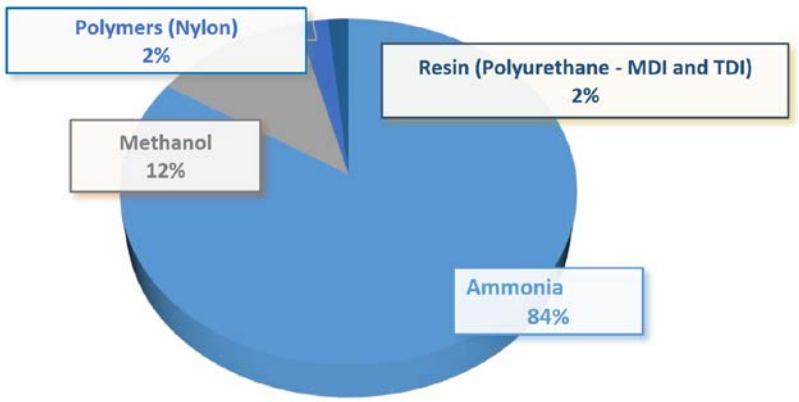


Figure 10: Main $H_2$ sub-consumers in the chemical industry. (Fraile et al., 2015)

Regarding the projections for the future, the chemical industry sector is less changing than e.g. the mobility sector. The ammonia market is expected to be relatively stable for the foreseeable future with an annual growth of about 0.1%. A similar outlook is obtained for methanol production. Only nylon is expected to increase its market share in the future with an annual growth of about 3.5-5% and is becoming a more and more competitive market. (Fraile et al., 2015)

## HYDROGEN PRODUCTION IN THE FUTURE

In the following, the planned hydrogen production for covering the rising demand will be presented for three exemplary areas, namely the United States, the EU 4 (Germany, Scandinavia, France, and UK) and Japan. Figure 11 shows a forecast of the hydrogen supply in those areas until 2050. These numbers were published by the Technology Roadmap for Hydrogen and Fuel Cells and differ from other values shown in this study. Nevertheless, Figure 12 gives a valuable insight into the future trend of the hydrogen supply for the three developed countries/regions United States, EU 4 and Japan. As it can be seen, the hydrogen supply will be heavily dependent on the fossil sources natural gas and coal. Carbon capture and sequestration (CCS) technologies are

planned to play an important role to reach climate goals. However, the amount of hydrogen from renewable sources should increase significantly as well. It becomes clear, that the hydrogen supply depends on regionally different resource endowments. While Japan only includes renewable electricity as source for renewable hydrogen, both the EU 4 and the United States plan to increase the production of hydrogen via biomass gasification significantly as well.

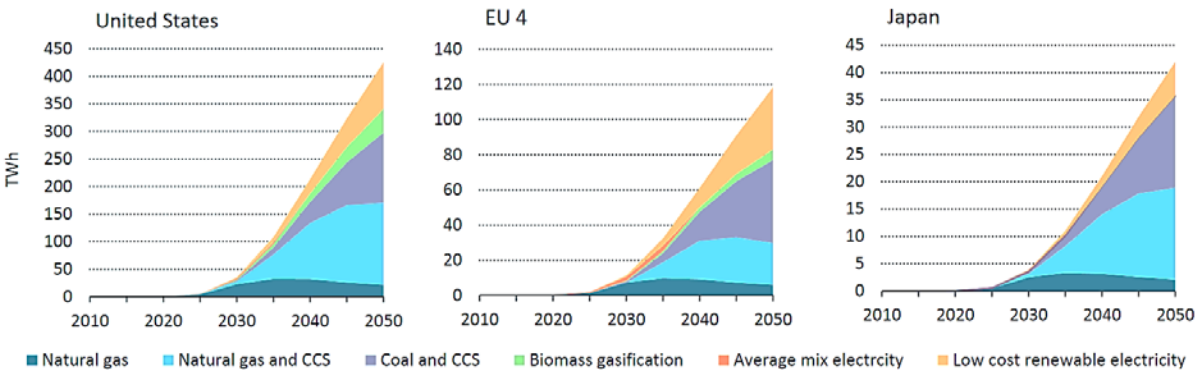


Figure 11: Hydrogen supply depends on regionally different resource endowments. (Technology Roadmap - Hydrogen and Fuel Cells, 2015)

In the following, the above mentioned uncertainty of the future market situation will be addressed. Figure 12 shows the expected annual cash flow projection for the next 10-15 years for the establishment of a hydrogen refueling network as a qualitatively concept. This is not solely related to hydrogen production, but shows the general challenge of establishing a new technology. Currently political framework conditions are not yet clear for the near future. They are however necessary to realize the planned increase in the production volume. The projected negative cash flow period for the next 10-15 years, until a more renewable-based hydrogen production can be established, needs political counter-measures in form of direct public support. As long as these political framework conditions are not defined and clear to the industry, projections for the future production will be in a state of uncertainty.

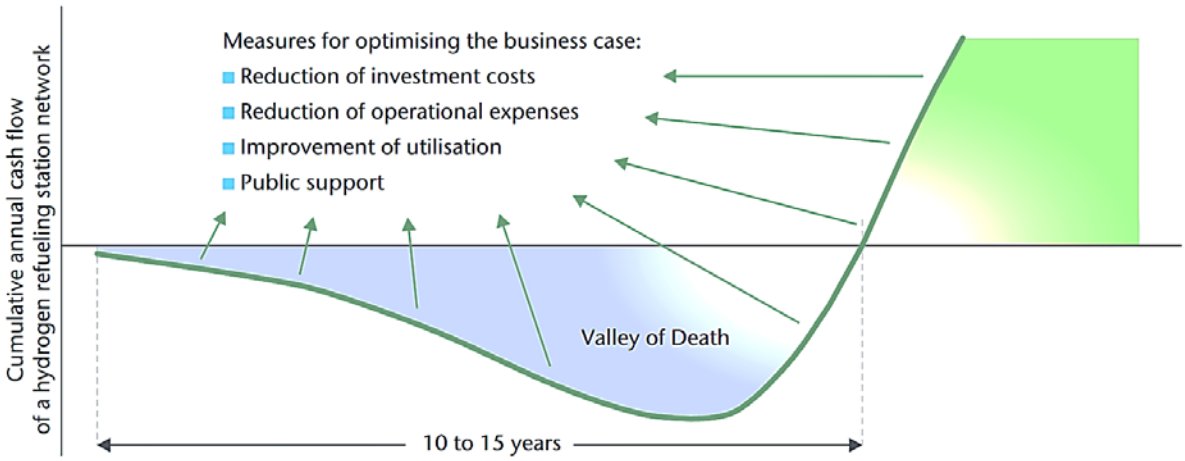


Figure 12: Expected annual cash flow projection for the next 10-15 years. (Technology Roadmap - Hydrogen and Fuel Cells, 2015)

In summary, it can be stated, that today's hydrogen market is dominated by the chemical industry and refining processes with a market share of above 90%. The production of hydrogen is based almost completely on fossil sources, whereas hydrogen production from renewable sources does not play a significant role yet. The projections for future hydrogen demand show that significantly higher production capacities will be needed to meet the rapidly increasing demand. Based on the goals to reduce greenhouse gas emissions, hydrogen from renewable sources as well as carbon capture and sequestrations technologies are needed in the future. Roadmaps of the United States of America and the EU 4 show, that hydrogen production based on biomass gasification is planned to play an important role in the providing hydrogen from renewable sources.

# Technology description

This chapter provides an overview of the state of the art principles of industrial hydrogen production and on hydrogen production based on biomass gasification. In general, hydrogen can be generated via the electrochemical, biochemical, and thermochemical route. All three routes enable $CO_2$-neutral hydrogen production. However, this study focuses on the thermochemical approach via gasification of biomass (wood chips). First, industrial hydrogen production is discussed, followed by biomass gasification with focus on fluidized bed gasification technologies.

The follows a section on the upgrading of the gases produced to clean hydrogen.

## INDUSTRIAL HYDROGEN PRODUCTION

This section gives an overview of the main industrial production technologies for hydrogen: steam reforming of natural gas, partial oxidation, coal gasification, and electrolysis.

**Steam reforming (SR)**, also referred to as steam methane reforming is the reaction of methane with steam in the presence of a catalyst to carbon monoxide and hydrogen, see Equation 1.

$$CH_4 + H_2O \leftrightarrow CO + 3\,H_2 \qquad \Delta H = +203\,\mathrm{kJ \cdot mol^{-1}} \qquad \text{Equation 1}$$

This reaction is strongly endothermic. In order to produce hydrogen, the synthesis gas exiting the reformer is usually subjected to a WGS unit (see subsection Water Gas Shift). Figure 13 illustrates the hydrogen production based on natural gas using SR with its main process steps.

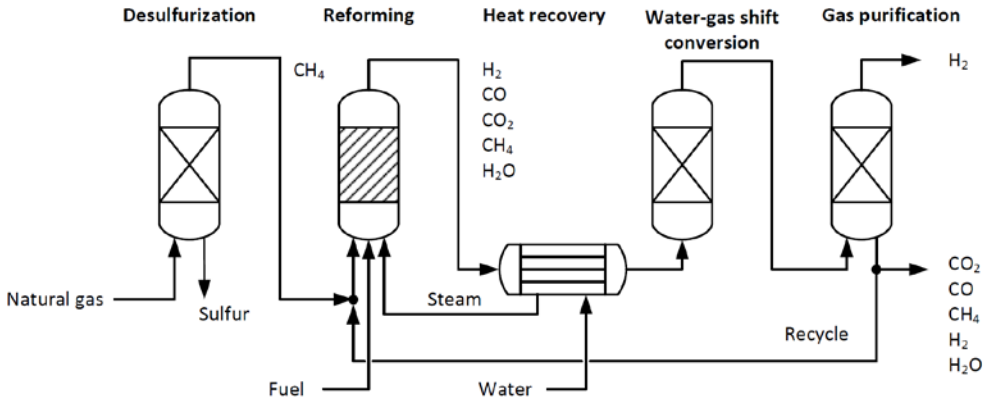


Figure 13: Hydrogen production using the steam reforming (SR) process with its process steps. (Díaz Pérez, 2013)

After desulfurization, steam reforming is carried out. Typical reaction conditions for steam reforming are at a temperature range between 500 to 900 °C. Because of the endothermic reaction, externally heating is needed. The pressure is usually at 20 bar and the steam to carbon ratio ranges from 2.5 to 3.0. Nickel-based catalysts have been favored, because of their sufficient activity and low cost. Consequently, the steps involved in the SR process for the production of

hydrogen can be divided into feed preparation, steam reforming, water gas shift (WGS) conversion, and hydrogen purification. (Liu et al., 2010)

The typical overall in generating hydrogen from natural gas by the SR process is approximately 50% on a LHV basis in the 0.15-15 MW range and up to 85 % in the 150-300 MW capacity range. (Körner, 2015)

Non-catalytic partial oxidation (POX), autothermal reforming (ATR), and catalytic partial oxidation (CPO) of hydrocarbon containing feedstock share the same chemical mechanism, which is shown in Equation 2 for the example of methane. These technologies are used in a wide range of scales but can be built at larger single-train units compared to SR.

$$CH_4 + \frac{1}{2}O_2 \leftrightarrow CO + 2\,H_2 \qquad \Delta H = -36\ \mathrm{kJ \cdot mol^{-1}} \qquad \text{Equation 2}$$

POX is the non-catalyzed reaction of natural gas or liquid hydrocarbons with oxygen at high temperature and high pressure to produce syngas. ATR is the reaction of natural gas or liquid hydrocarbons with steam and oxygen at high temperature and high pressure to produce syngas. The reaction is exothermic and catalysts are used to improve hydrogen yield. CPO is the heterogeneous reaction of natural gas or liquid hydrocarbons with oxygen and steam at high space velocity over a solid catalyst to produce syngas. (Liu et al., 2010) Figure 14 illustrates those different partial oxidation processes, including further downstream process steps aiming for hydrogen production.

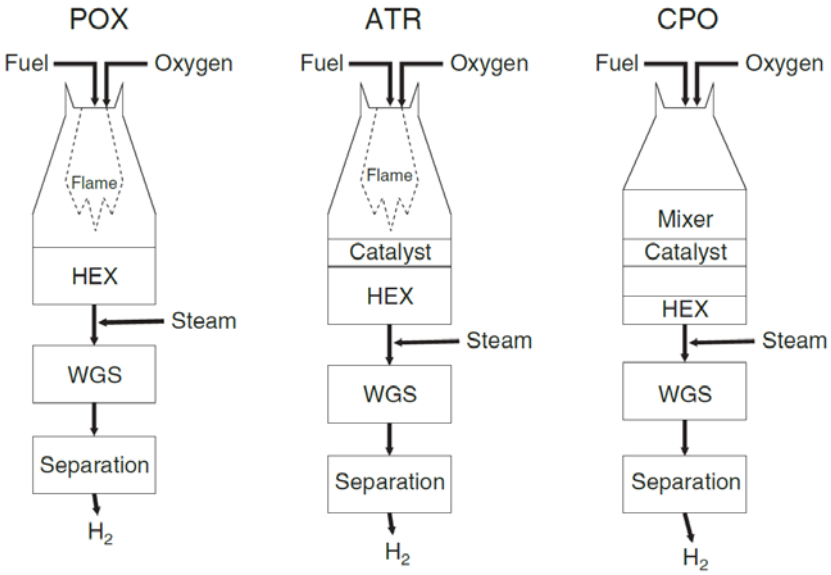


Figure 14: Schematic representation of non-catalytic partial oxidation (POX), autothermal reforming (ATR), and catalytic partial oxidation (CPO) reformers. Heat exchanger (HEX). (Liu et al., 2010)

In contrast to steam reforming, the partial oxidation reaction is slightly exothermic. The

technological differentiation of reforming comes from the method by which the heat is generated and provided. For CPO or ATR, a portion of the fuel is oxidized within the reactor to generate the heat required to drive the endothermic steam reforming reaction occurring over the same catalyst bed. The main advantage of the partial oxidation process is that it will produce a synthesis gas with a favorable hydrogen to carbon monoxide ratio for downstream usage in chemical syntheses. In order to produce pure hydrogen the process will also include a WGS unit and a hydrogen purification step. (Liu et al., 2010)

**Coal gasification** is a well-established technology to convert coal with steam and oxygen to a synthesis gas which generally consists of CO, $H_2$, $CO_2$, $CH_4$, higher hydrocarbons, and impurities such as $H_2S$ and $NH_3$. Coal gasifiers combust some of the coal with $O_2$ to provide the heat for the gasification reactions, this is referred to as autothermal gasification. Steam or carbon dioxide is added to enhance gasification reactions. (Liu et al., 2010) Coal gasification with pure oxygen as gasification agent can be seen as partial oxidation of a solid fuel. A schematic flow diagram of coal gasification and its main applications is shown in Figure 15. Coal gasification processes are more often used in conjunction with producing chemicals like e.g. ammonia and methanol, than for pure hydrogen.

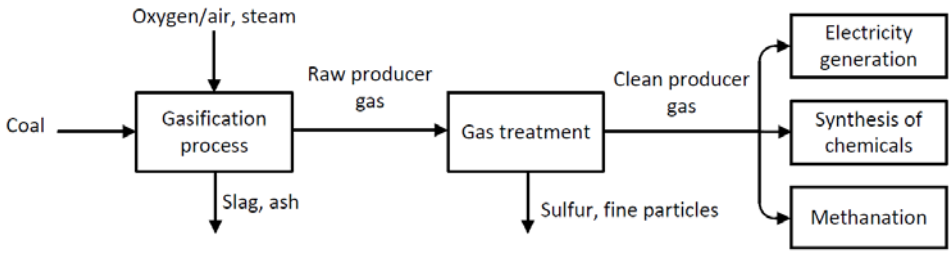


Figure 15: Basic process steps of coal gasification and its main applications. (Díaz Pérez, 2013)

Hydrogen can be obtained from **electrolysis** of water by using electrical power. If electricity comes from renewable sources, electrolysis could be a promising technology for future renewable hydrogen production. However, electrolysis is currently used in a much smaller scale compared to steam reforming. (Liu et al., 2010)

One benefit of electrolysis is the possible integration into a power-to-gas system used as energy storage. With power-to-gas, excess electricity is converted into hydrogen and oxygen by water electrolysis. The hydrogen can be stored and reconverted into electricity using fuel cells, or used as feedstock for further syntheses as well as secondary energy carrier. Also the oxygen should be brought to a commercial exploitation.

Electrolyzer technologies, operating from atmospheric up to 1 MPa pressure, can be divided into alkaline, PEM, and solid oxide electrolysis cells, according to the electrolyte which is applied. (Gahleitner, 2013) Figure 16 shows the main process steps of hydrogen production using

electrolysis or even power-to-gas applications. In the case of electrolyzers, high-purity hydrogen is produced directly, and only drying and compression is required to arrive at normal merchant quality. The typical efficiency of electrolyzers is in the 50-70 % range, depending on the electrolyzer.

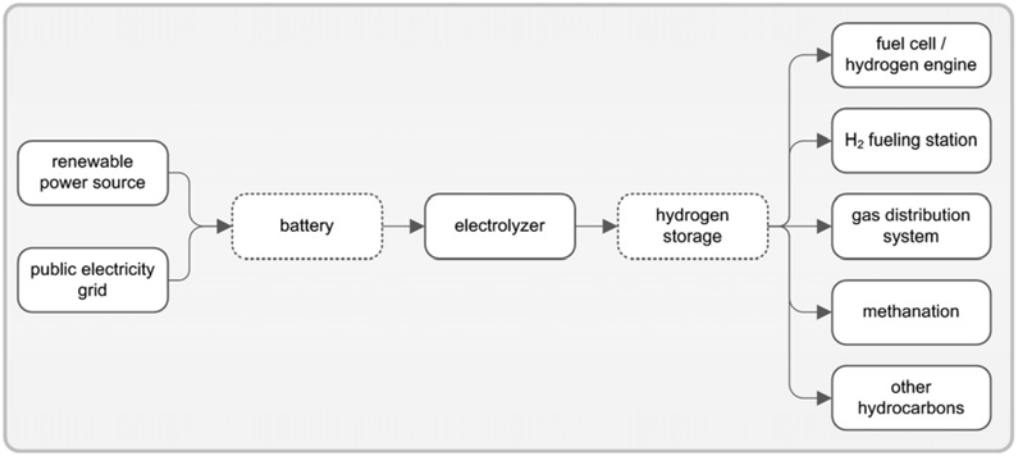


Figure 16: Process chain of the hydrogen production based on electrolysis. (Gahleitner, 2013)

## BIOMASS GASIFICATION

Gasification is the thermochemical conversion of a carbonaceous solid fuel into a product gas (also referred to as producer gas, or in the case of wooden feedstock referred to as wood gas) in the presence of a specific gasification agent. Figure 17 shows a general process layout for hydrogen production via gasification.


Figure 17: General process layout for hydrogen production via gasification.

Suitable technologies for the production of hydrogen, which are available for the single process steps, will be addressed in this study. Gas cleaning and upgrading is necessary in order to remove bulk CO and $CO_2$ as well as trace components like $H_2S$, $NH_3$, HCl, and tar. Separating benzene, toluene, ethylbenzene, and xylene (BTEX) is not necessary as it is usually removed with the $H_2$ separation equipment.

Figure 18 illustrates biomass in a C-H-O-diagram. There exist different strategies or pathways for

performing the conversion from feedstock towards products within gasification, as illustrated in Figure 18 by a-e, each marked with arrow. Adding steam as a gasification agent is common practice, not only due to the stoichiometric effect, but also for enhanced char gasification and temperature moderation within the reactor. (Schildhauer and Biollaz, 2016)

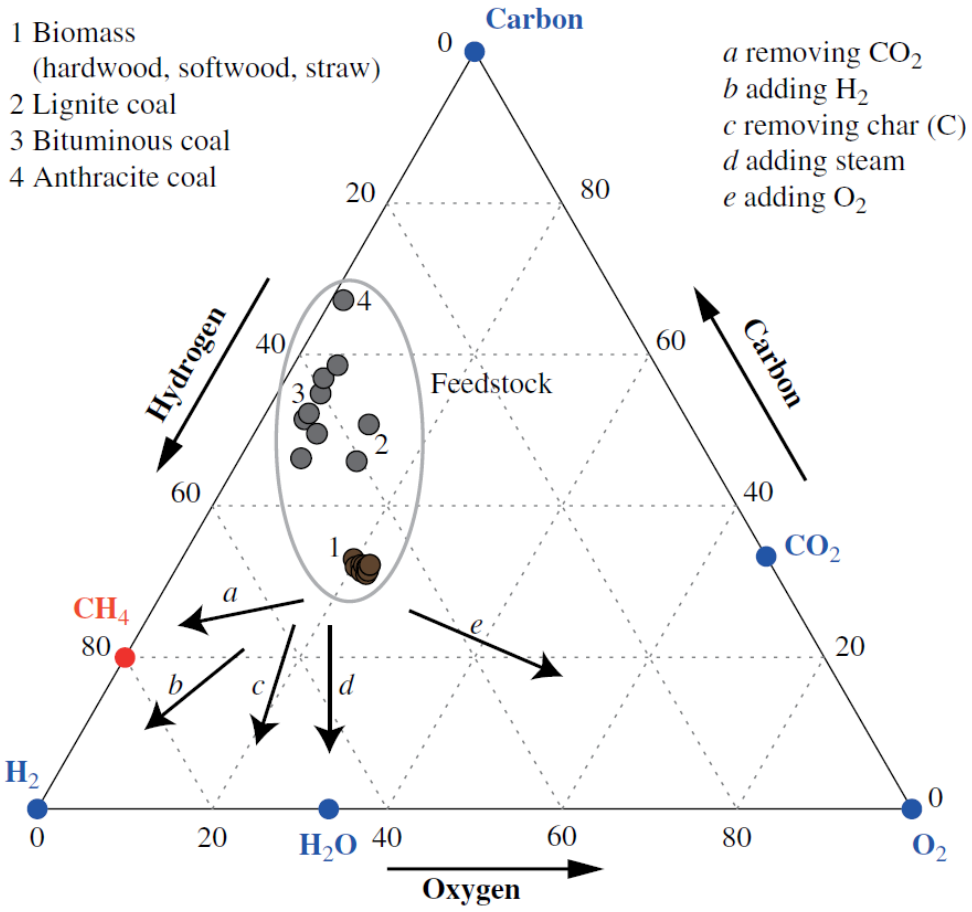


Figure 18: C-H-O-diagram for coal and biomass. (Schildhauer and Biollaz, 2016)

Gasification of biomass offers a great potential of possible product gas applications and there are various gasification technologies available for biomass. The main difference is the used gasification agent and related to this the way of heat supply, which is necessary because of the overall endothermic gasification reactions. This heat can be either added externally, in a so called allothermal gasification process, or generated internally by the full combustion of some biomass, referred to as autothermal gasification process. Another defining feature at different gasification processes is the reactor design, which distinguishes between fixed bed, fluidized bed, and entrained flow reactors and the used gasification agent. In general, gasification is comprised of several steps (Kaltschmitt et al., 2016; Liu et al., 2010):

- Evaporation of moisture at temperatures up to 150 °C
- Pyrolysis, therefore releasing of volatiles ($H_2$, CO, $CO_2$, $CH_4$, tar, etc.) between 200 and 650 °C
- Reaction of volatiles in the gas phase between 700 and 1 000 °C
- Heterogeneous reaction of char between 700 and 1 000 °C

During the gasification process, mainly the following homogeneous (Equation 3 - Equation 7) and heterogeneous (Equation 8 - Equation 14) reactions take place (compare (Kaltschmitt et al., 2016; Liu et al., 2010)). Based on these equations, the following gasification agents can be identified: $O_2$, $H_2O$, $CO_2$, and $H_2$. The reactions displayed here cover the most important gasification reactions; however it has to be kept in mind, that other reactions such as pyrolysis or volatiles reacting after their release do also play a significant role in the gasification process.

Heterogeneous gasification reactions:

$$C + O_2 \leftrightarrow CO_2 \qquad \Delta H = -394\ kJ \cdot mol^{-1} \qquad \text{Equation 3}$$

$$C + \frac{1}{2}O_2 \leftrightarrow CO \qquad \Delta H = -111\ kJ \cdot mol^{-1} \qquad \text{Equation 4}$$

$$C + H_2O \leftrightarrow CO + H_2 \qquad \Delta H = +119\ kJ \cdot mol^{-1} \qquad \text{Equation 5}$$

$$C + CO_2 \leftrightarrow 2\ CO \qquad \Delta H = +160\ kJ \cdot mol^{-1} \qquad \text{Equation 6}$$

$$C + 2\ H_2 \leftrightarrow CH_4 \qquad \Delta H = -88\ kJ \cdot mol^{-1} \qquad \text{Equation 7}$$

Homogeneous gasification reactions:

$$CO + H_2O \leftrightarrow CO_2 + H_2 \qquad \Delta H = -41\ kJ \cdot mol^{-1} \qquad \text{Equation 8}$$

$$CO + 3\ H_2 \leftrightarrow CH_4 + H_2O \qquad \Delta H = -203\ kJ \cdot mol^{-1} \qquad \text{Equation 9}$$

$$CO_2 + 4\ H_2 \leftrightarrow CH_4 + 2\ H_2O \qquad \Delta H = -162\ kJ \cdot mol^{-1} \qquad \text{Equation 10}$$

$$CO + \frac{1}{2}O_2 \leftrightarrow CO_2 \qquad \Delta H = -283\ kJ \cdot mol^{-1} \qquad \text{Equation 11}$$

$$H_2 + \frac{1}{2}O_2 \leftrightarrow H_2O \qquad \Delta H = -242\ \mathrm{kJ \cdot mol^{-1}}$$ Equation 12

$$2\ CO + 2\ H_2 \leftrightarrow CH_4 + CO_2 \qquad \Delta H = -244\ \mathrm{kJ \cdot mol^{-1}}$$ Equation 13

$$CO_2 + 2\ H_2O \leftrightarrow CH_4 + 2\ O_2 \qquad \Delta H = +790\ \mathrm{kJ \cdot mol^{-1}}$$ Equation 14

In general, for autothermal gasification, either air, pure $O_2$, or a mixture of $O_2$ and steam can be used. Therefore, the heat for the endothermal gasification reactions is supplied by partial combustion of the fuel. If air is employed as gasification agent, the resulting product gas is highly diluted by nitrogen. In this case, the product gas has only a low calorific value around 4 to 6 MJ·m$^{-3}$ because of a high nitrogen content of 45 to 55%. In case of the allothermal gasification, steam or $CO_2$ or a combination of both is used as gasification agent. In order to supply the heat for the endothermic gasification reactions, either a heat pipe or a circulating bed material, as it is employed in the dual fluidized bed or in the sorption enhanced reforming process, can be used.

In case of hydrogen production, it is necessary to produce a $N_2$ free product gas, so air gasification processes are neglected in this study. However, in the following, only allothermal gasification processes generating a $N_2$ free product gas are investigated. The reason is that the focus is on medium to small scale plants, where allothermal gasification systems are advantageous.

Different twin bed gasification systems have been developed over the years. Concepts include Batelle, Ferco, Rentech, and the Milena Gasifier by ECN (which will be addressed later on). In the following, more specific description will be presented for selected technologies.

### Dual fluidized bed gasification technology from TU Wien

The basic idea of the so called dual fluidized bed (DFB) gasification concept, developed primarily at TU Wien, Austria, is to divide the gasification process into two separated zones. The gasification reactor, where the gasification with steam, in the absence of oxygen takes place, is separated from the combustion reactor which provides the heat necessary for endothermic gasification. The gasification reactor is operated as a bubbling fluidized bed and is fluidized with steam, which acts as well as gasification agent. The combustion reactor is operated with air as a fast fluidized bed. Char is transported together with bed material from the gasification to the combustion reactor, where is exothermically burns and produces heat. The bed material is thus heated up and a circulation loop of bed material between these two reactors ensures that heat, which is needed for the gasification process, is transported from the combustion to the gasification reactor. Fluidized loop seals ensure that wood gas from gasification and flue gas from combustion remain separated. This leads to a nearly nitrogen free wood gas with a calorific value of more than 12 MJ·m$^{-3}$.

(Hofbauer et al., 2002; Kaltschmitt et al., 2016) Figure 19 shows the principle of the DFB gasification technology for producing a $N_2$ free product gas.

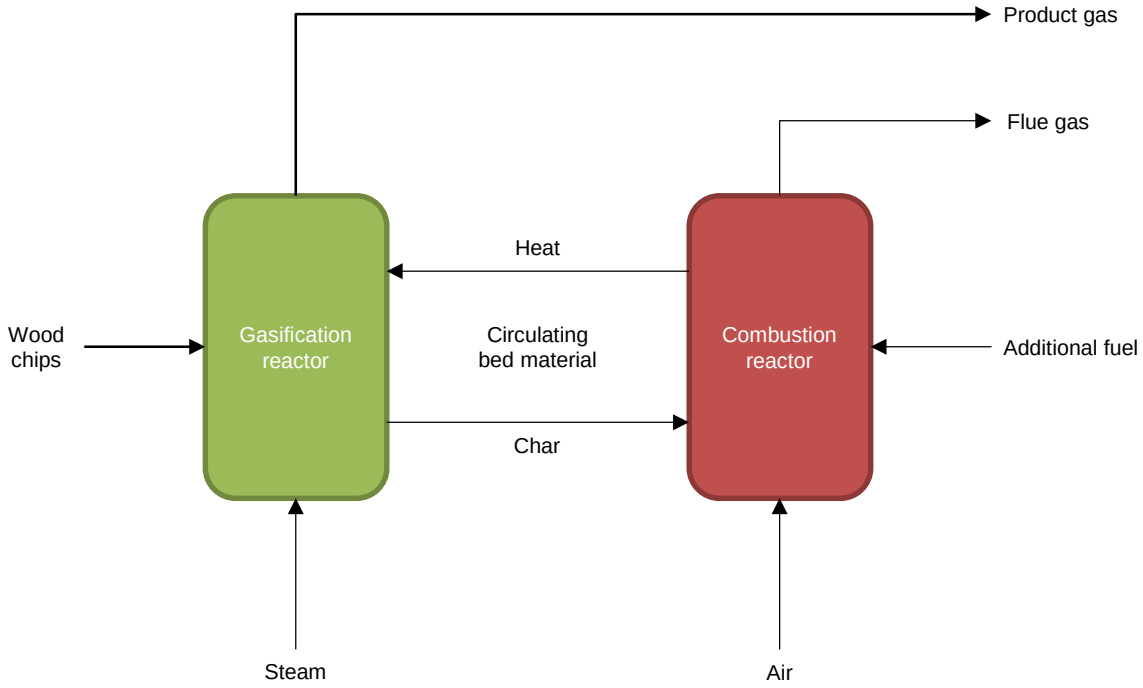


Figure 19: Principle of DFB steam gasification of biomass.

The gas velocities in the gasification reactor are comparably slow to increase the residence time for the gasification reactions. However, other concepts have been developed with other reactor configurations. There are different DFB concepts evolving, e.g. ECN has proposed a DFB reactor concept with a circulating bed gasification reactor and a bubbling fluidized bed combustion reactor. In (Corella et al., 2007) there is a detailed overview about DFB gasification.

Today, at industrial scale, olivine is used as bed material. The olivine bed material has two major roles. Firstly, it is a heat carrier, as described above, to provide the heat from the combustion to the gasification reactor. Secondly, it acts as catalyst in the gasification reactor to promote the gasification reactions, such as the steam reforming of hydrocarbons (lighter hydrocarbons and tar) or the WGS reaction. (Kirnbauer and Hofbauer, 2013; Kuba et al., 2016) When using olivine, commercial plants using woody biomass as feedstock achieve a volumetric $H_2$ content of about 40%.

Table 1 shows the product gas composition, which can be achieved, if woody biomass is used as feedstock and olivine as bed material.

Table 1: Typical product gas composition of the DFB gasification.(Kaltschmitt et al., 2016)

| Components | Values | Units |
|---|---|---|
| $H_2$ | 35-45% | $m^3 \cdot m^{-3}$ |
| CO | 22-25% | $m^3 \cdot m^{-3}$ |
| $CO_2$ | 20-25% | $m^3 \cdot m^{-3}$ |
| $CH_4$ | about 10% | $m^3 \cdot m^{-3}$ |
| $C_2H_4$ | 2-3% | $m^3 \cdot m^{-3}$ |
| Tar (incl. BTEX) | 20-30 | $g \cdot m^{-3}$ |

It can be seen, that the $H_2$:CO ratio ranges from about 1.5:1 up to 2:1. This ratio is a good basis for synthesis reactions, for example methanol or Fischer-Tropsch (FT) synthesis.

The first demonstration-scale plant of the DFB technology was realized as a combined heat and power (CHP) plant in Güssing, Austria. The Güssing plant was operated for a total of about 15 years and has produced important scientific and industrial knowledge for the further development of the technology. The CHP principle based on the DFB technology was used for several other commercial plants.

Currently, most of the commercial plants are not operating due to changes in the ownership or decisions to terminate the commercial operation. At this point it is expected, that at least two of the commercial plants will start up their operation again in the near future. Today, the plant in Senden/Ulm, Germany is the state-of-the-art of commercial DFB gasification as it successfully operates with logging residues rich in needles and leaves as feedstock.

Figure 20 shows a simplified flowchart of the employed CHP process in Güssing, Austria. The product gas leaving the reactor is cooled down to temperatures below 200 °C before passes through a filter, where fly char is separated from the gas stream. Afterwards, the product gas enters into a scrubber unit for condensation of $H_2O$ and separation of condensable tar from the product gas. The scrubber is operated with rapeseed methyl ester (RME), in which the condensable tar is adsorbed. The emulsion of tar and bio-oil is not discharged from the system as waste stream, but is brought into the combustion reactor, where it is combusted and provides

additional energy to the system. The product gas is then led to a gas engine where it produces electricity and district heat.

The flue gas leaving the cyclone is also cooled down and filtered from the fine ash fraction. The energy recycled from the heat exchangers is internally used for steam generation or externally used as district heat.

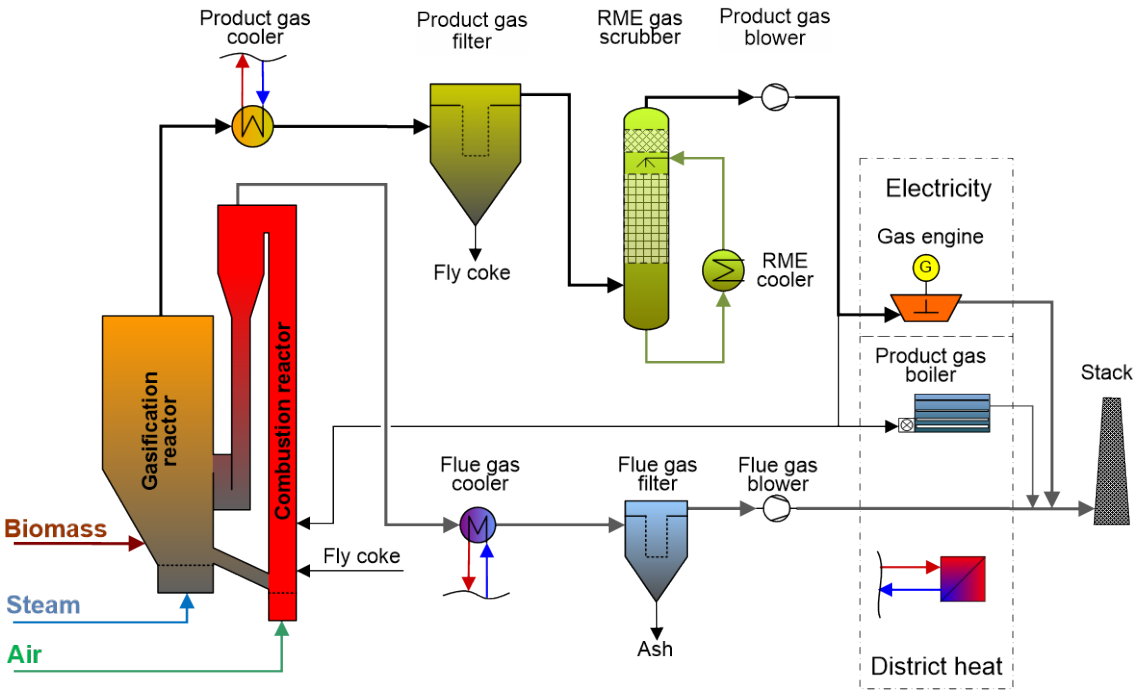


Figure 20: Flowchart of the commercial DFB plant in Güssing, Austria. Based on (Hofbauer et al., 2002).

## MILENA gasification technology

The principle of the MILENA gasifier, which was mainly developed by the Energy research Centre of the Netherlands (ECN), is similar to that of the DFB technology. The MILENA gasifier is also a system applying two fluidized beds, as shown in Figure 19. However, the gasification reactor is operated as a fast fluidized bed, whereas the combustion reactor is operated as a bubbling fluidized bed (BFB). Figure 21 shows a schematic representation of the MILENA gasification reactor. The gasification reactor is realized as a riser, where the bed material is entrained together with the feedstock particles. After the riser the particles are separated from the product gas stream and brought down to the bubbling fluidized bed reactor zone via the downcomer (or settling) section. (Van der Drift et al., 2005)

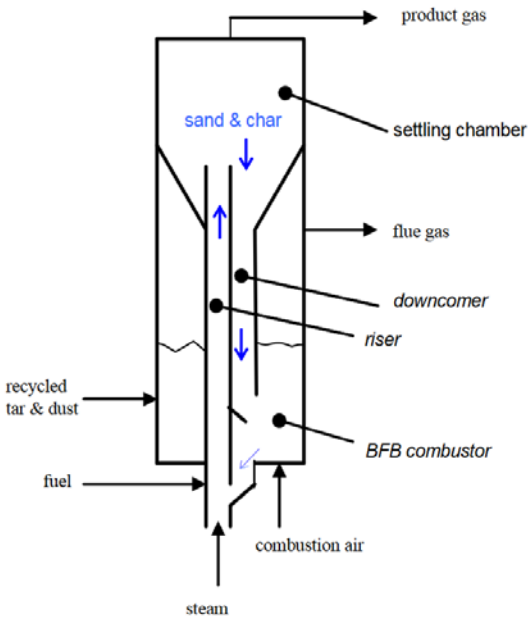


Figure 21: Schematic principle of the MILENA gasification reactor.(Van der Meijden et al., 2008a)

In comparison to the DFB system, here less steam is necessary as gasifying medium, which leads to a higher cold gas efficiency (CGE) of the system. However, in the fast fluidized bed gasification reactor the residence time of the product gas and the catalytically active bed material is lower in comparison to the residence time in the bubbling fluidized bed reactor used in the DFB system. Thus, the volatiles from the biomass and formed tar components have less contact time with the catalytic active material which is disadvantageous for reducing tar components in the product gas.

(Van der Meijden et al., 2008b) published a concept for a 10 $MW_{th}$ demonstration plant based on the MILENA gasification technology. Figure 22 shows a simplified scheme of the reactor concept for the demonstration plant. The upscaling of the reactor to demonstration-scale was realized through implementing a second settling chamber. In the configuration quartz sand or olivine were foreseen as possible bed materials.

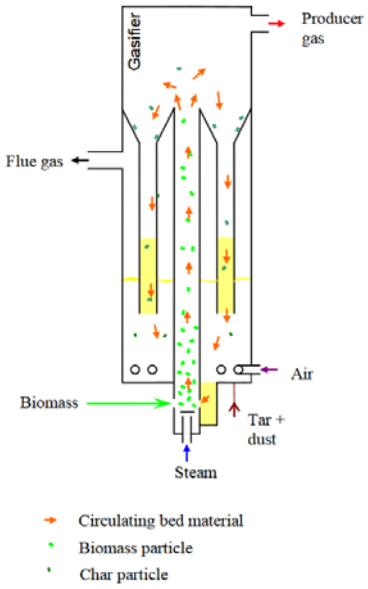


Figure 22: Simplified scheme of MILENA gasifier. (Van der Meijden et al., 2008b)

Typically gas compositions for steam gasification with the MILENA technology, when using Austrian olivine as bed material, are presented in Table 2. As it can be seen, a volumetric hydrogen fraction of around 27–28% can be achieved at a gasification temperature of around 800 °C.

Table 2: Typical product gas composition of the MILENA gasification. (Van der Meijden et al., 2008b)

| Components | Values | Units |
|---|---|---|
| $H_2$ | 27-28% | $m^3 \cdot m^{-3}$ |
| CO | 27-28% | $m^3 \cdot m^{-3}$ |
| $CO_2$ | 24-25% | $m^3 \cdot m^{-3}$ |
| $CH_4$ | 9-10% | $m^3 \cdot m^{-3}$ |
| Tar (incl. BTEX) | 18-20 | $g \cdot m^{-3}$ |

Figure 23 shows the schematic flow sheet of the 800 $kW_{th}$ pilot plant, which is currently in operation at the ECN research facility in the Netherlands. Gas cleaning is achieved through the, so called OLGA system, which is similarly to the DFB technology based on an oil-scrubber for removal of tar components. OLGA employs an additional tar adsorption and regeneration step, resulting in clean gas, which can be used in engines or turbines. At the pilot plant the product gas from gasification is burned in a boiler. (Van der Meijden, 2010)

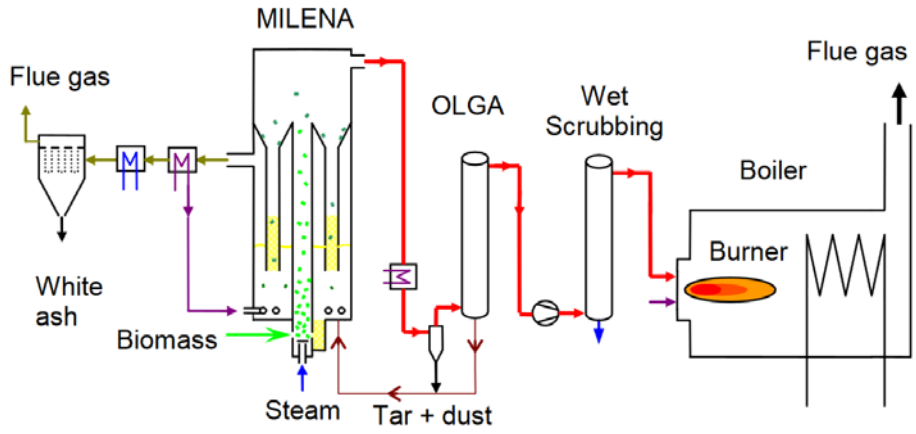


Figure 23: Basic layout of the 500 $kW_{th}$ pilot plant. (Van der Meijden, 2010)

The ECN MILENA and OLGA technology are now commercially available through a joint venture between ECN and Dahlman Renewable Technology (DRT).

## Heat-pipe reformer technology

The heat-pipe reformer is also an allothermal gasification technology, however it differs significantly from the two above mentioned systems, as the heat transfer from combustion to gasification is achieved through heat pipes instead of circulating bed material. Furthermore, the gasification reactor, or heat-pipe reformer as it is called in this configuration, is a pressurized vessel which operates between 2-10 bar and 800 °C. (Karl, 2014)

Figure 24 shows a process scheme of the heat-pipe reformer. The heat necessary for the gasification is supplied by a combustion reactor (2) which is located underneath the gasification reactor. Heat pipes (3) are connecting the two reactors. Those heat pipes are filled with a carrier medium, which is evaporated in the combustion reactor. Thus the evaporated medium transports the heat from the combustor to the gasifier where the medium condensates and releases the heat. To ensure a sufficiently high heat transfer between both the combustion and the gasification reactor are operated as bubbling fluidized beds. The feedstock is added through a stand pipe (6). Steam (5) is also added from the top.

Thus, even though this technology differs significantly from the two above mentioned concepts, it is also biomass steam gasification based on fluidized bed reactor systems, which can be used for the production of hydrogen.

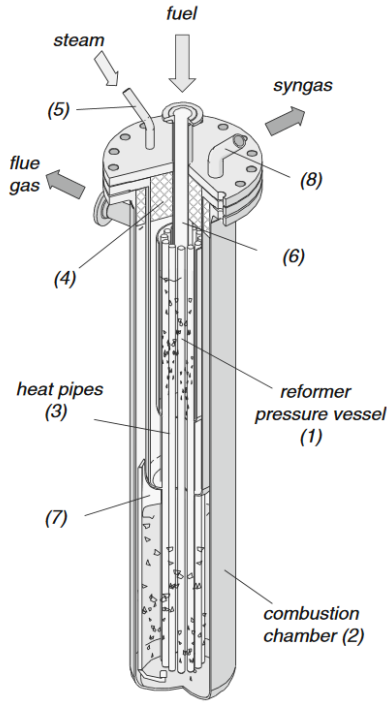


Figure 24: Conceptual design of the biomass Heat-Pipe reformer. (Karl, 2014)

Table 3 shows the typical composition of the product gas, which is achieved with the heat-pipe reformer. As shown, the volumetric $H_2$ fraction in the product gas reaches values of above 40%.

Table 3: Typical product gas composition of the heat-pipe reformer. (Karl, 2014)

| Components | Values | Units |
|---|---|---|
| $H_2$ | 40-46% | $m^3 \cdot m^{-3}$ |
| CO | 18-22% | $m^3 \cdot m^{-3}$ |
| $CO_2$ | 20-26% | $m^3 \cdot m^{-3}$ |
| $CH_4$ | 8-12% | $m^3 \cdot m^{-3}$ |
| Tar (excl. BTEX) | 1-8 | $g \cdot m^{-3}$ |

Figure 25 shows a schematic illustration of the heat-pipe reformer test-rig, which is currently operated in the laboratory of the University of Erlangen-Nuremberg, at the Institute of Energy Process Engineering. The fluidized bed combustor is made of refractory concrete and is able to withstand the temperatures and abrasive conditions of the bubbling fluidized bed. The flue gas enters an annular gap between the heat exchanger and the gasification reactor and is cooled down while it is preheating the primary and secondary air. (Karl, 2014)

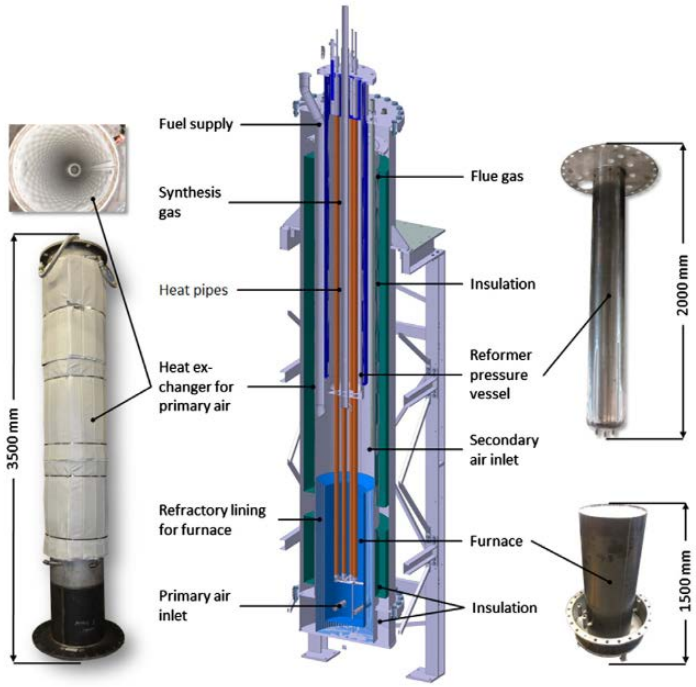


Figure 25: Laboratory set-up of the heat-pipe reformer at the Department of Chemical and Bioengineering of the Friedrich Alexander-University Erlangen-Nürnberg

Other allothermal gasification systems are also investigated in research projects, but are less developed than the above mentioned technologies and are therefore not yet relevant in the discussion of hydrogen production in commercial scale. Moreover, most of the developments are based on similar principles than those above and therefore, the overview will not include other systems.

### Sorption enhanced reforming

The sorption enhanced reforming (SER), sometimes referred to as adsorption or absorption enhanced reforming (AER), can reach higher $H_2$ contents by the selective removal of $CO_2$ from the reactive zone in the gasifier which pushes the equilibrium of the WGS reaction to the side of hydrogen. Consequently, a volumetric $H_2$ content of about 75% can be reached with SER. Figure 26 shows the principle of the SER process. There are instrumental similarities between the DFB gasification process and the SER, both applying two fluidized beds and a circulating loop of bed material. In the case of the SER process limestone, $CaCO_3$, is used as bed material.

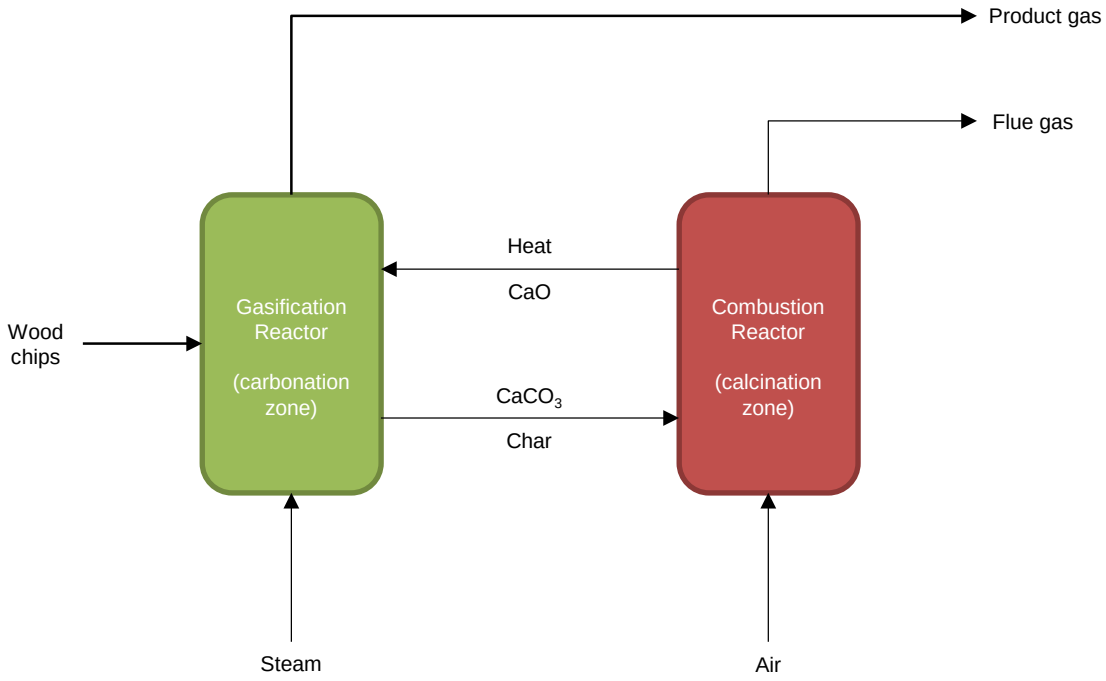


Figure 26: Principle of SER process based on biomass.

In addition to other bed materials, $CaCO_3$ serve as $CO_2$ carrier, which leads to an in-situ $CO_2$ removal from the product gas. This is achieved by the circulating bed material. CaO reacts with $CO_2$ in the gasification reactor at about 650-700 °C according to Equation 15.

$$CaO + CO_2 \leftrightarrow CaCO_3 \qquad \Delta H = -178\ kJ \cdot mol^{-1} \qquad \text{Equation 15}$$

The formed $CaCO_3$ is transported to the combustion reactor were it is regenerated again to CaO, releasing the $CO_2$, at about 900 °C. Compared to olivine, CaO shows higher catalytic activity resulting in a higher $H_2$ content and a lower tar content of the product gas. However, its mechanical stability is lower compared to olivine and abrasion causes significantly higher bed material losses compared to olivine.

Three institutions investigated SER with different plants. TU Wien at a 100 kW (fuel) DFB gasifier, University of Stuttgart at a 200 kW (fuel) DFB gasifier, and the commercial biomass steam gasification plant in Güssing, Austria. All plants which were used for the experimental investigations are based on the DFB biomass steam gasification technology described above. (Fuchs et al., 2017; Hawthorne et al., 2012; Müller, 2013; Norman Poboß, 2016; Pfeifer et al., 2009) Based on these data, Table 4 shows typical product gas composition of the SER process.

In (Hawthorne et al., 2012), (Pfeifer et al., 2009), and (Norman Poboß, 2016), experimental investigations and in (Müller, 2013) a process simulation with the commercial software IPSEpro

based on experimental results was carried out. In (Fuchs et al., 2017) experimental investigations based on a new DFB gasifier design was carried out, this new design also enhances the suitability in terms of SER operation. However, even the SER process shows similarities to the DFB process regarding the reactor concept; no demonstration plant is yet available. Only pilot-scale experiments have shown successful operation so far.

Table 4: Typical product gas composition of the SER process.

| Components | Values | Units |
|---|---|---|
| $H_2$ | 73% | $m^3 \cdot m^{-3}$ |
| CO | 8% | $m^3 \cdot m^{-3}$ |
| $CO_2$ | 6% | $m^3 \cdot m^{-3}$ |
| $CH_4$ | 11% | $m^3 \cdot m^{-3}$ |
| $C_xH_y$ | 2% | $m^3 \cdot m^{-3}$ |
| Tar (excl. BTEX) | ~10 | $g \cdot m^{-3}$ |

## PRODUCT GAS UPGRADING AND CLEANING

This section gives an overview about state of the art unit operations which can be used for upgrading and cleaning of biomass derived product gas to produce hydrogen, with focus on technologies, applied in the section; investigated hydrogen production routes.

### Water gas shift

In order to increase the $H_2$ yield and to lower the CO content of the generated product gas, a WGS unit is employed. The WGS reaction, shown in Equation 16, is a well-established technology in industrial large-scale plants producing hydrogen or setting the CO/H2 ratio of synthesis gas.

$$CO + H_2O \leftrightarrow H_2 + CO_2 \qquad \Delta H = -41.2\ kJ \cdot mol^{-1} \qquad \text{Equation 16}$$

The WGS reaction converts carbon monoxide and steam to hydrogen and carbon dioxide. Its equilibrium constant decreases with temperature, therefore, high conversions are favored by low temperatures, as shown in Figure 27. (Liu et al., 2010)

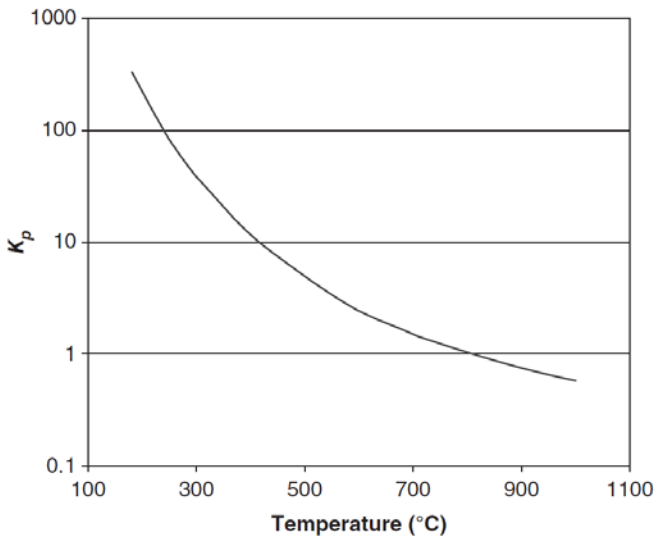


Figure 27: Variation of equilibrium constant (Kp) for the water gas shift reaction with temperature. (Liu et al., 2010)

At the industrial scale, a WGS unit is usually one or more fixed bed reactors. For a relatively small CO conversion for adjustment of the $CO/H_2$ ratio for synthesis a by-pass high temperature (HT) WGS stage is sufficient, whereas for producing $H_2$, the fuel gas stream is treated in 2-3 stages at gradually lower inlet and outlet temperature to achieve a high CO conversion.

In order to reach economic reaction rates, different catalysts can be used. Fe-Cr-based catalysts are suitable for a HT WGS stage. This HT stage operates adiabatically with a gas inlet temperature of 350 to 550 °C and space velocities from 400 to 1 200 $h^{-1}$. The operating pressure depends on the plant requirements. (Liu et al., 2010) Fe-Cr-based catalysts seem to be robust against sulfur

poisoning at the orders of magnitude of $H_2S$ which are observed in the product gas of biomass steam gasification. (Fail, 2014; Twigg, 1989) Catalysts for the low temperature (LT) stage (about 200 °C) are Co-Mo or Cu-Zn-based catalysts. The Co-Mo catalyst is resistant to the presence of sulfur components but the amount of $H_2S$ in the product gas of biomass steam gasification is too low for the Co-Mo catalyst to reach a high level of activity as the Co-Mo catalyst is activated by sulfur (compare (Chianese et al., 2016; Fail, 2014)). In contrast, Cu-Zn catalysts are very sensitive to sulfur poisoning (Liu et al., 2010), therefore sulfur removal would be necessary. This section focuses on the Fe-Cr-based catalyst as it has proofed very suitable for the operation with the product gas from DFB biomass steam gasification. (Chianese et al., 2015; Fail et al., 2014; Michael Kraussler et al., 2016)

The Fe-Cr-based HT shift catalyst is composed of $Fe_3O_4$ and $Cr_2O_3$, basically the same catalyst as developed by BASF in 1915. The catalyst is relatively inexpensive, because of the $Cr_2O_3$ resistant to sintering and robust against sulfur and chlorine compounds. (Zhu and Wachs, 2016) give an extensive review of iron-based high temperature water gas shift catalysts.

One key factor which affects the performance of the Fe-Cr-based WGS catalyst and influences the overall heat integration of a plant is the steam to dry gas ratio at the reactor inlet. Both, laboratory and commercial data indicate that higher steam to dry gas ratios also increase the water gas shift reaction rate. As a result of the steam to dry gas ratio's effect on the thermodynamic and kinetic properties of the process, higher values give higher CO conversions and a lower exit CO content in the gas. In addition to the CO conversion, the steam to dry gas ratio can also affect the production of hydrocarbons (mainly methane) by the FT reaction. In order to minimize such undesirable reactions, a minimum steam to dry gas ratio of 0.4 should be ensured at the inlet of a WGS reactor. In addition, a certain amount of steam prevents the risk of coking and carbon deposition on the catalyst's surface. Depending on the feed of the WGS reactor, typical molar steam to dry gas rations are between 0.6 and 2.2, steam to carbon ratios between 2.8 and 4.2. (Ratnasamy and Wagner, 2009) Figure 28 shows the ternary C-H-O-diagram for 1 bar, indicating if coking and carbon deposition is thermodynamically favored.

In the last years, several experiments were carried out with a WGS pilot plant consisting of three fixed bed reactors in series, which employed a commercial Fe-Cr-based catalyst (Shiftmax 120 from the company Clariant). The same catalyst batch was operated for more than 3 000 hours with the product gas from the commercial DFB biomass steam gasification plant Oberwart, Austria, of which more than 2 200 hours with tar-rich product gas extracted after the product gas filter of the plant. (Fail et al., 2014; Michael Kraussler et al., 2016)

In addition (M. Kraussler et al., 2016) compared the operation of the WGS pilot plant with product gas extracted before and after the RME scrubber. No significant performance differences could be observed. In both cases, operated adiabatic with a gas temperature of 350 °C at the reactor inlet, a CO conversion rate of at least 91% was achieved and the volumetric CO fraction at the outlet of the pilot plant was lower than 2%. Those results indicate that a WGS unit can be operated with filtered but tar-rich product gas extracted after the filter and before the RME scrubber of a DFB biomass steam gasification plant.

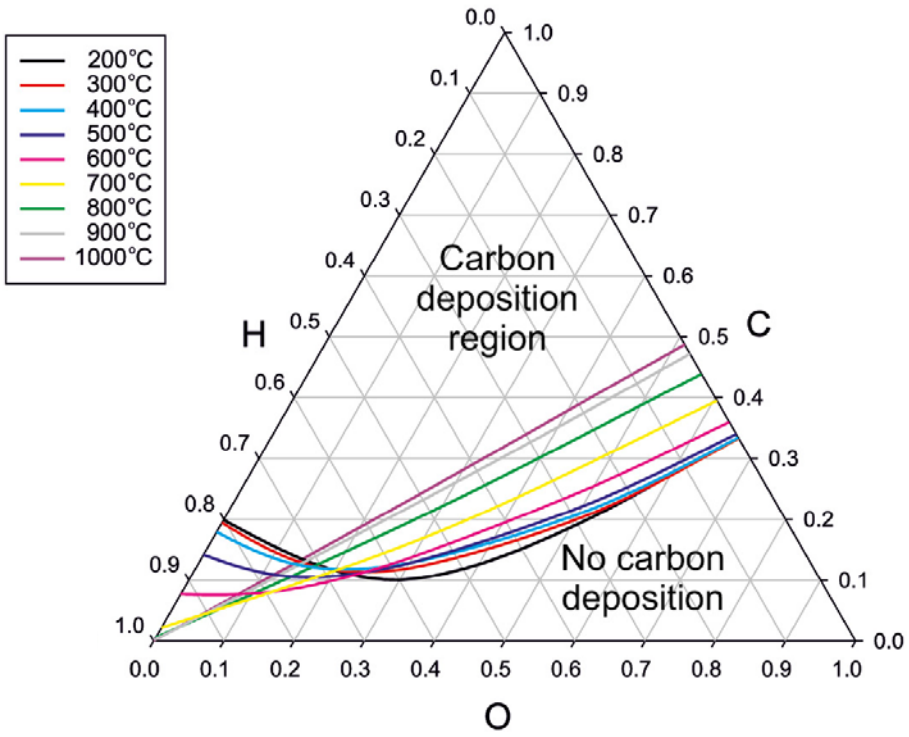


Figure 28: Ternary C-H-O-diagram for solid phase of all carbon allotropes at 1 bar. (Jaworski et al., 2017)

WGS catalysts also have a hydrogenation effect on other components in the gas such as e.g. HCN and olefins, and the sulfur-equivalent reaction of transferring COS to $H_2S$.

### Rapeseed oil methyl ester tar scrubber

The product gas generated by the DFB gasification system contains a significant amount of tar. Tar is an undesired by-product of gasification as it may negatively affect a downstream unit or catalyst. In order to remove the tar and to condense the steam by lowering the gas temperature, a wet scrubber can be employed. Using RME as organic solvent in the wet scrubber has been well proven at the commercial DFB plants in Güssing and Oberwart, Austria and Senden, Germany (Kuba et al., 2018; Pröll et al., 2007; Wilk and Hofbauer, 2016), as well as at the GoBiGas plant in Sweden (Thunman et al., 2018).

Typically RME scrubbers are built as scrubber units filled with structured packings. Cooled RME wets the packings while flowing downwards and is thus in good contact with the product gas which is passing in counter-current mode. Due to the contact with the cooled RME, the temperature of the product gas is significantly reduced below the water dew point. Thus, water, which absorbs part of the ammonia from the product gas, condenses. The separation of the emulsion of condensate and RME is realized in the scrubber basin below the scrubber itself. Due to the density

difference between water condensate and RME the separation is achieved in a first step. A part of the condensate –specific heavier condensate – is not separable from the oily RME and is collected at the lower part of the basin. Thus, the lower part is filled halfway with condensate. The remaining emulsion is separated from the rest and is burnt in the combustion chamber, where it provides energy as additional fuel. No waste stream needs to be discharged from the system. (Bardolf, 2017)

(Bardolf, 2017) summarizes the state of the art and latest research results regarding the RME scrubbing units employed at commercial DFB plants serving tar removal and steam condensation. (Thunman et al., 2018) discusses the experience of the RME scrubber, at the GoBiGas plant. Therefore, in all investigated processes the RME scrubber was employed to remove tar. It was assumed that the scrubber operating temperature is 50 °C, therefore, tar is partially removed (tar content decreased from 5 to 1.5 $g \cdot m^{-3}$) and steam condensed.

### Amine scrubber

Amine scrubbing has been used to separate carbon dioxide from gaseous streams since 1930. (Rochelle, 2009) The $CO_2$-rich gas stream is contacted with an aqueous amine solution. The amine solvent reversibly reacts with $CO_2$ forming water-soluble salts. Amine-based solvent processes are well-suited to capture $CO_2$ from dilute low pressure streams. (MacDowell et al., 2010) Problems during operation can occur due to the corrosive behavior of amines, formation of non-soluble salts, and foaming. (Klinski, 2006)

Due to the high affinity of especially $CO_2$ to the used solvents, mainly aqueous solutions of monoethanolamine (MEA), diethanolamine (DEA) and methyldiethanolamine (MDEA), the operating pressure of amine scrubbers can be kept at ambient level. The high capacity and high selectivity of the amine solution turns out to be a disadvantage during the regeneration of the scrubbing solution. Chemical scrubbing liquids require a significant amount of energy for the regeneration which has to be provided as process heat. As a small part of the scrubbing liquid is lost due to evaporation, it has to be replenished frequently. Hydrogen sulfide could also be chemically absorbed but higher temperatures during regeneration would be needed. (TVT TU Wien, 2012)

The loading capacity for chemical solvents like amines is primarily dependent on the concentration of the active components and the achievable loading according to the thermodynamic equilibrium. For the range of alkanolamines, the primary amines (MEA) will be more favorable in terms of reaction rates compared to secondary (DEA), or tertiary (MDEA) amines. However, achievable loadings and heat requirement for regeneration will be also higher for primary amines. (Bailey and Feron, 2005)

Today, the most common industrially used amine system is a mixture of MDEA and piperazine (PZ), often termed activated MDEA (aMDEA). aMDEA uses piperazine as a catalyst to increase the speed of the reaction with $CO_2$. This system is today supplied by several major suppliers of chemicals such as BASF, DOW chemicals, Shell, and Taminco. (Bauer et al., 2013; Meerman et al., 2012; Solutions, 2011) In general, different solvents show the following $CO_2$ removal efficiency: water < MDEA < DEA < MEA. With PZ activated MDEA seems to have the same $CO_2$ removal efficiency as MEA, but seems to be less corrosive. Furthermore, the energy requirements of MDEA are usually lower compared to MEA and DEA. (Privalova et al., 2013) Figure 29 shows the principle of an amine scrubbing unit with amine regeneration.

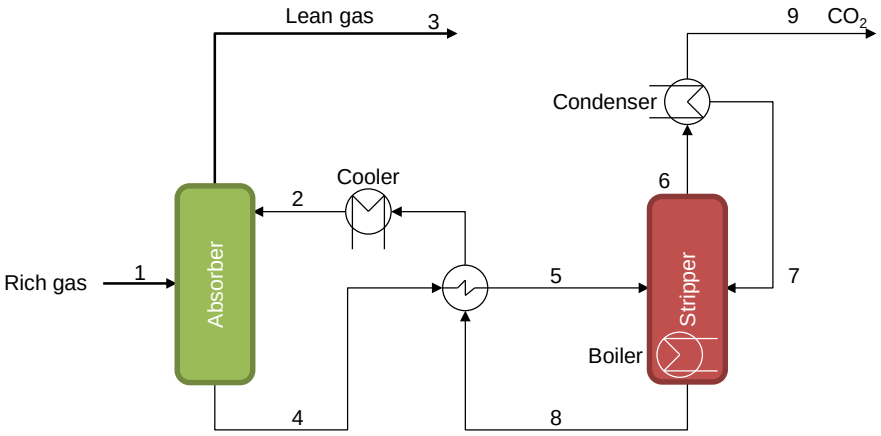


Figure 29: Simplified flowchart of an amine scrubbing process. Based on (Bauer et al., 2013).

The $CO_2$ rich gas stream (1) is fed into the absorber where the $CO_2$ reacts with the amine solution resulting in the lean gas stream (3). The liquid amine solution (referred to as lean amine with a low $CO_2$ content) enters from the top of the absorber (2) and leaves at the bottom (4, rich amine). The rich amine is then preheated and enters the stripper (5). In the stripper, the rich amine solution flows in counter-current flow down to the bottom. At the bottom, the aqueous amine solution is heated up in order to desorb $CO_2$ and to generate steam, which heats the rich amine solution falling from the top of the column. The steam and the desorbed $CO_2$ leave the stripper at the top (6). Subsequently, the steam and a small part of evaporated amine is condensed and fed back to the stripper (7), whereas the $CO_2$ leaves the stripper (9). The regenerated amine solution (8) is cooled and used again in the absorber (2).

According to (Bauer et al., 2013), amine scrubbers can reach $CO_2$ removal efficiencies of up to 99.8% with biogas with a volumetric fraction of 40% $CO_2$ in the feed. (Ryckebosch et al., 2011) report $CO_2$ removal efficiencies up to 99.5%. Further $CO_2$ purification would bring the $CO_2$ quality up to food-grade standard. (Bailey and Feron, 2005)

Table 5 shows typical operating parameters of amine scrubber. The operating conditions depend on the $CO_2$ concentration in the feed and the used amine solvent.

Table 5: Typical operating parameters of amine scrubbers.

| Parameters | Values | Units | Sources |
|---|---|---|---|
| Stripper temperature | 100 to 160 | °C | (Bauer et al., 2013; Rochelle, 2009; TVT TU Wien, 2012; Urban et al., 2009; Wang et al., 2011) |
| Absorber temperature | 40 to 65 | °C | Bauer et al., 2013; Urban et al., 2009; Wang et al., 2011) |
| Electricity demand | 300 to 700 | $kJ \cdot kg^{-1}$ absorbed CO2 | Bauer et al., 2013; Romeo et al., 2008; Scholz et al., 2013; Starr et al., 2012; Thrän et al., 2014) |
| Heat for regeneration | 1 400 to 4 000 | $kJ \cdot kg^{-1}$ absorbed CO2 | (Bauer et al., 2013; Knudsen et al., 2009; Persson, 2013; Romeo et al., 2008; Scholz et al., 2013; Thrän et al., 2014) |
| Solvent consumption | 0.35 to 2 | $kg \cdot t^{-1}$ absorbed CO2 | (Bailey and Feron, 2005; Knudsen et al., 2009; Starr et al., 2012) |

### Catalytic hot gas cleaning for tar reduction

Product gas from gasification processes is characterized by certain amounts of undesired condensable hydrocarbons, also referred to as tar. Other than using scrubbers to separate the tar components from the gas stream, there have been published numerous studies on reduction of tar at high temperatures (~ 800 °C) using catalysts. This field has received significant attention from the scientific community and main results from the experience with catalytic hot gas cleaning for tar reduction will be discussed in the following section.

First, catalytic reformers downstream of the gasification reactor have been investigated in detail. Whereas the utilization of ceramic monoliths has been observed to be challenging due to the critical operational conditions (high dust loads, high temperature peaks, etc.), the utilization of metal-based monoliths has been successfully tested in commercial-scale. The gasification plant in Skive, Denmark, is using a reforming unit based on metal monoliths as tar reduction step directly downstream of the gasification reactor.(Andersson et al., 2017) A schematic display of the tar reformer monolith in Skive is shown in Figure 30. (Voss et al., 2016) Long-term operation with satisfactory results has been established. In such a tar reformer the product gas is not cooled

down beforehand and passes at around 800 °C through the reformer. The surface of the supporting monolith is catalytically active (usually through catalytically active coatings) and tar is reformed through the reaction with steam.

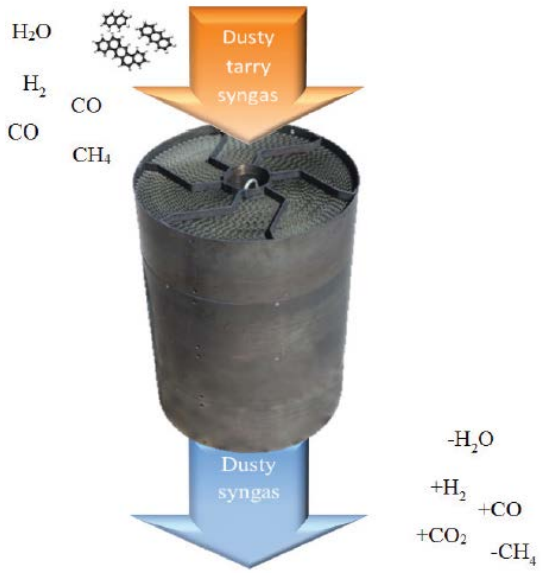


Figure 30: Illustration of the tar reformer monolith in Skive, Denmark.(Voss et al., 2016)

For synthesis gas processing, to reform both tar and methane, Haldor Topsoe and Andritz-Carbona have developed both a monolithic, dirty reformer catalyst and a clean dumped catalyst to operate upstream or downstream particulate removal, respectively. These were tested for extended periods at pilot plant scale at Gas Technology Institute. (GTI, 2015)

Another approach to catalytic hot gas cleaning for the reduction of tar is the utilization of catalytically active filter candles. Here both dust and tar are reduced in only one process step. The underlying principle is similar as the product gas is separated from tar at about 800 °C. Such catalytic filter candles can be employed directly in the freeboard above a fluidized bed reactor. The positioning of the combined dust and tar reducing gas cleaning within the gasification reactor itself results in a comparably compact unit. (Rapagnà et al., 2012) The research in the past years has mostly focused on the material of the candle itself to withstand the challenging operational conditions in fluidized bed gasification. The reducing atmosphere in steam gasifiers as well as the comparably high load of dust and particles which is entrained from fluidized beds has posed a significant challenge. Figure 31 shows images of catalytic filter candles, which were tested in 22 h test-runs in a fluidized bed reactor. (Rapagnà et al., 2010)

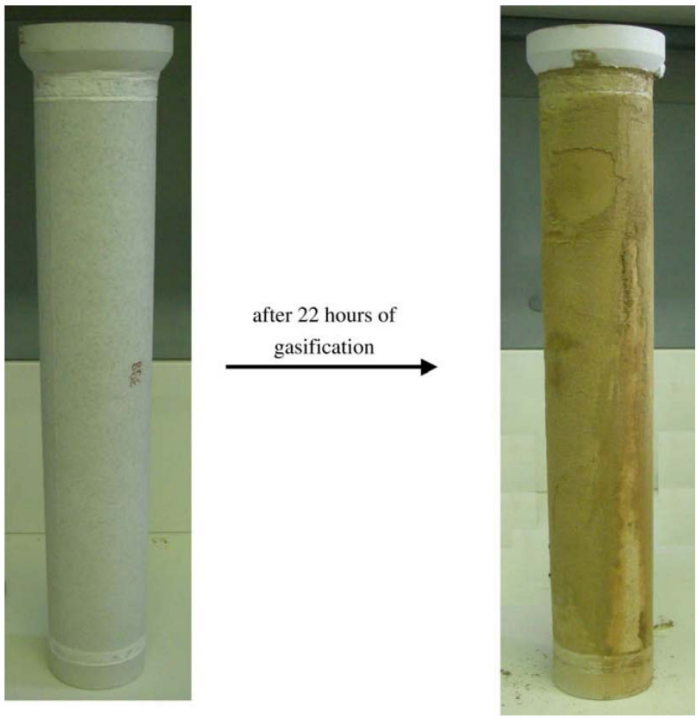


Figure 31: Catalytic ceramic candle before and after the gasification test. (Rapagnà et al., 2010)

## Dust filters

Typically in commercially available gasification installations dust is separated from the product gas stream with conventional bag house filters. Thus the product gas needs to be cooled down below 200 °C to ensure the durability of the bag house filter. Residual char particles entrained from the gasification reactor together with the product gas are collected in the filter. Depending on the gasification technology, the so called fly char is then either returned internally (e.g. into the combustion reactor in a dual fluidized bed system) or discharged from the system as waste stream.

Another possibility to separate dust particles from the product gas is the utilization of electrostatic precipitators (ESP). ESPs are especially advantageous for removing small dust particles. The particles are separated from the gas stream by using the force of an induced electrostatic charge. ESPs are currently employed in commercial plants and are e.g. used in certain fluidized bed air gasification reactors. However, the high carbon content of the fly coke from gasification makes ESPs problematic as downstream cleaning. Wet ESPs (WEP) are a suitable alternative for cooling and condensing to remove aerosols of solids or liquids.

As already mentioned above, high-temperature filters such as filter candles, have been also investigated in detail.

### Further gas cleaning

Depending on the used feedstock further gas cleaning might be necessary. As this is specific to feedstock issues and not directly related to hydrogen production, which is the focus of the present study, further gas cleaning concepts will not be discussed. In addition, a comprehensive literature study on hot gas cleaning with a focus on catalytic processes was published in the frame of the master's thesis of (Kuba, 2013).

## HYDROGEN SEPARATION TECHNOLOGIES

PSA and membrane based processes have been investigated. However, if high purity is needed (> 99%) a PSA process is necessary.

### Pressure swing adsorption

PSA process is based on the physical binding of gas molecules to a solid adsorbent material. The interaction between the gas and the adsorbent depends mainly on the gas component, its partial pressure, the type of adsorbent, and the temperature. It is a state of the art process for gas separation and widely used at commercial scale for different applications, for example air separation, hydrogen production, and biogas upgrading. (Miltner, 2010; Sircar, 2002; TVT TU Wien, 2012) Figure 32 shows a simplified flowchart of a PSA process.

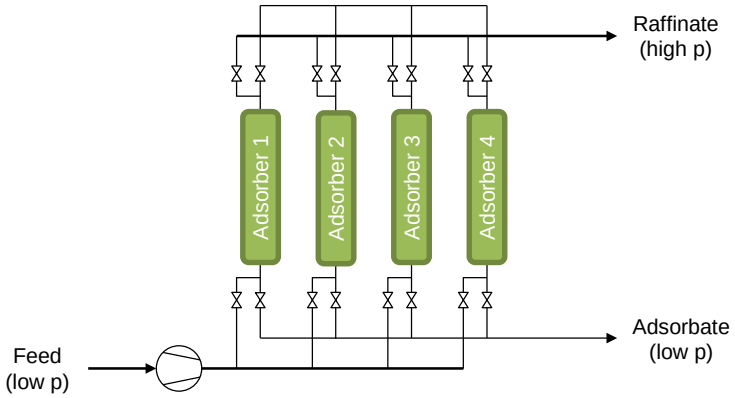


Figure 32: Simplified flowchart of a PSA process.

The feed is compressed and successively fed into the different adsorber vessels. The vessels, which are not in contact with the feed, are regenerated by lowering the pressure and flushing with high-pressure product (raffinate). The low-pressure product (adsorbate) which contains the contaminants of the feed can be reused within upstream or downstream processes.

Considering the main gas components of the processed gas, the adsorption strength on activated carbon can be described by the following relation: $CO_2$ > $CH_4$ > CO > $H_2$. (Liu et al., 2010) This means that $CO_2$ is preferably adsorbed on the activated carbon and, hence better removed from

the feed gas stream than, for example $H_2$. Consequently, activated carbon is a suitable adsorbent for the production of pure $H_2$.

In the last years, several approaches aiming to reach the fuel cell grade $H_2$ production via PSA from product gas derived from DFB biomass steam gasification plants were carried out at the sites of the DFB plants in Güssing and Oberwart, Austria. During these experiments with a lab-scale PSA unit employing activated carbon as adsorbents, $H_2$ recoveries up to 80% were reached. (Díaz Pérez, 2013; Fail et al., 2014)

With additional $CO_2$ separation before the PSA unit and further optimization measures, 90% $H_2$ recovery can be achieved. However, there is always a trade-off between $H_2$ recovery and $H_2$ purity. In addition, the adsorbate should be considered, which can be internally recycled, or e.g. be used for fuel. Therefore, if high grade $H_2$ (purity higher than 99.999%) should be generated, the recovery could be significantly lower. (Liu et al., 2010)

## Gas permeation through membranes

As applied to gas separations, membrane - based processes are nearly always pressure - driven separation processes, similar to PSA, which has enjoyed significant commercial success. However, unlike PSA, membrane processes are typically continuous throughput rather than cyclical in nature and membrane processes are usually more easily controlled. A membrane is a discrete, thin interface that moderates the permeation of chemical species in contact with it. This interface may be molecularly homogeneous or heterogeneous. A basic representation of a membrane gas separation system is shown in

Figure 33, where a membrane is sealed within a housing (pressure vessel) to make a membrane module. A gas stream (feed) enters the membrane system where it is split in two fractions: raffinate and permeate. The permeate fraction is richer in gas molecules that permeate easier through the membrane (e.g. hydrogen). (Liu et al., 2010)

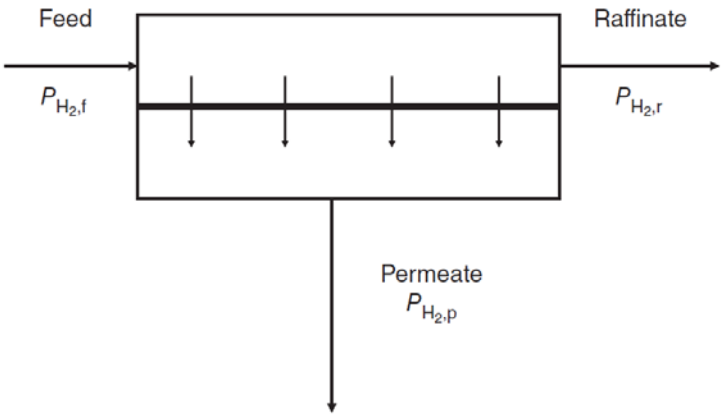


Figure 33: Schematic of a hydrogen separation membrane and membrane module. (Liu et al., 2010)

There are essentially four different types of membranes, or semipermeable barriers, which have either been commercialized for hydrogen separations or are being proposed for development and commercialization. They are polymeric membranes, porous (ceramic, carbon, metal) membranes, dense metal membranes, and ion - conductive membranes, see Table 6. Of these, only the polymeric membranes have seen significant commercialization. (Liu et al., 2010)

Table 6: Comparison of Membrane Types for Hydrogen Separation. (Liu et al., 2010)

| Parameters | Membrane Type | | | |
|---|---|---|---|---|
| | **Polymeric** | **Nanoporous** | **Dense Metal** | **Ion Conducting** |
| Typical composition | Polyimide; cellulose acetate | Silica; alumina; zeolites; carbon | Palladium alloys | Water-swollen, strong-acid, cation exchange membranes; dense ceramics (perovskytes) |
| Diffusion mechanism | Solution-diffusion | Size exclusion | Solution-diffusion | Solution-diffusion |
| Driving force | Pressure gradient | Pressure gradient | Pressure gradient | Ionic gradient |
| Operating temperature in °C | ≤110 | ≤1000 | ≤150-700 | ≤180 (polymeric); 700-1000(ceramic) |
| Relative permeability | Moderate-high | Low-moderate | Moderate | Moderate |
| Typical selectivity | Moderate | Low-Moderate | Very high | Very high |
| Relative cost | Low | Low | Moderate | Low |

## INVESTIGATED HYDROGEN PRODUCTION ROUTES

Based on the $H_2$ production pathway described by (Arregi et al., 2018), see Figure 1, and based on experimental experiences gathered in (Fail et al., 2014; Kraussler et al., 2017; Michael Kraussler et al., 2016), two process layouts for hydrogen from biomass gasification concepts are presented; a DFB gasification based, as well as, a SER based $H_2$ production route. Both routes deliver hydrogen at 10 bar and a purity of 99.97%. The SER process does not employ an amine scrubber and a WGS unit, as $CO_2$ is in-situ removed during the gasification, which enhances the WGS reaction already in the gasification reactor.

In terms of $H_2$ capacities, two scales were considered, according to the market requirements; On one hand a small (1 MW $H_2$ capacity) scale SER based process, which does not include PSA adsorbate recycle. On the other hand a medium (50 MW $H_2$ capacity) scale DFB based process. For this process, the PSA adsorbate, which is rich in $CH_4$, is fed into a steam reforming unit to convert the $CH_4$ into additional CO and $H_2$. Subsequently, the gas stream is recycled into the process before the WGS unit. This increasing complexity and additional steam is required, on the other hand the $H_2$ yield is maximized.

### Employed unit operations

This section introduces the chosen operating conditions and assumptions which were used to derive the mass- and energy-balance. Based on this data basis, the techno-economic assessment was carried out.

Gasification: DFB and SER were unpressurized and for both the gasification reactor was operated with steam and the combustion reactor was operated with air. Wood chips were chosen as feedstock, arriving with moisture content of 40%, and to be fed into the gasification with moisture content of 20%.

The CGE (see Equation 17) was assumed to be 77%, and in the case of DFB, excluding the recycle into the combustion reactor. The biomass is considered before drying (40% moisture).

$$\mathrm{CGE} = \frac{\mathrm{LHV}_{\mathrm{Biomass}}}{\mathrm{LHV}_{\mathrm{Productgas}}} \qquad \text{Equation 17}$$

WGS: The water gas shift reactor was calculated as equilibrium reactor minimizing the Gibbs enthalpy without kinetic data. For the simulation of the water gas shift reactor only CO, $H_2O$, $H_2$, and $CO_2$ were considered as reactive components. The inlet temperature was around 350 °C and the reactor was assumed to be adiabatic. The steam content was set, using a ternary C-H-O diagram, to achieve conditions where coking and carbon deposition is thermodynamically not

favored, compare (Jaworski et al., 2017). According the ternary C-H-O diagram (see Figure 34), the steam content at the WGS unit inlet was set to a S/CO ratio of 3.4, corresponding to a S/C ratio of 1.7.

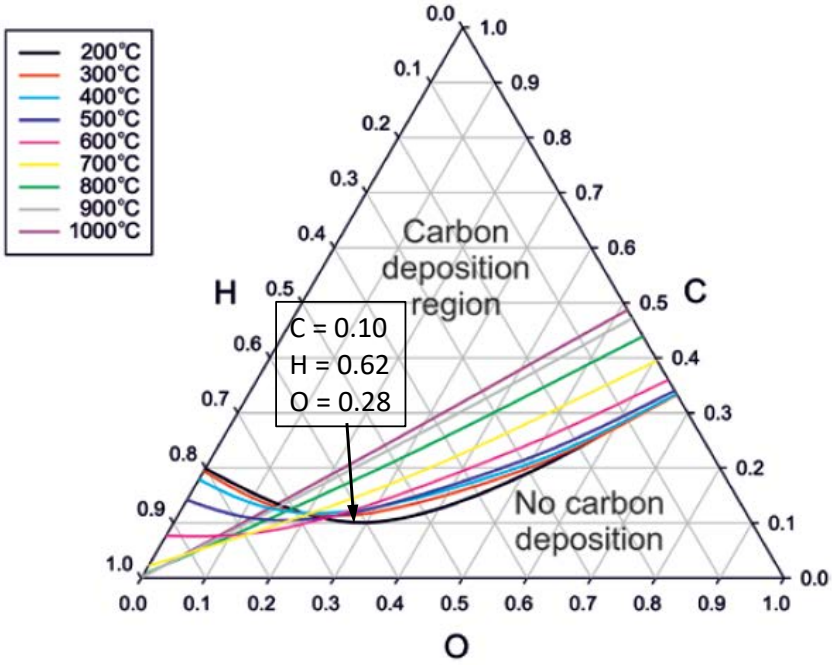


Figure 34: C-H-O-ternary diagram for p = 1 bar, indicating the C-H-O-ratio of the gas at the inlet of the WGS unit, operated with DFB gasification derived product gas. Based on (Jaworski et al., 2017).

RME scrubber: It was assumed that the gas stream leaves the RME scrubber with a temperature of 50 °C and saturated with moisture, compare (Bardolf, 2017). According to (Jünger, 2008), the excess heat of the RME scrubber can be utilized in an low-temperature-level dryer, which is used to dry the biomass from a moisture content of 40%down to am moisture content of 20%.

Amine scrubber: aMDEA was selected as solvent and a $CO_2$ removal efficiency of 99% was chosen, compare (Bauer et al., 2013; Ryckebosch et al., 2011). Furthermore, based on (Bauer et al., 2013; Tobiesen et al., 2007) a thermal consumption of 2.4 MJ and an electricity consumption of 0.4 MJ per kg adsorbed $CO_2$ was assumed.

PSA: During PSA test runs, employing activated carbon as adsorbents, processing real product gas from biomass gasification, hydrogen recoveries up to 80% were reached. (Fail et al., 2014) With additional $CO_2$ separation downstream the PSA unit and further optimization measures, 90% hydrogen recovery can be achieved. (Liu et al., 2010) In this work, a Hydrogen recovery of 85% and a hydrogen purity of 99.97% were assumed. The PSA was operated with a pressure of 10 bar, which was also assumed to be pressure the produced hydrogen is provided. The adsorbate was assumed to be depressurized.

SR: The steam reforming reactor was calculated as equilibrium reactor minimizing the Gibbs enthalpy without kinetic data. For the simulation of the reforming reactor only $CH_4$, $C_2H_4$, $C_2H_6$, $H_2O$, CO, and $H_2$ were considered as reactive components. The reactor was calculated as isothermal at a temperature level of 850 °C. The S/C ratio was set to 2.5, compare (Liu et al., 2010). In addition, the steam content was verified using a ternary C-H-O diagram. However, for a S/C ratio of 2.5 the operating point is in the area where coking and carbon deposition is thermodynamically not favored, compare (Jaworski et al., 2017).

The sulfur content in the product gas, which is originated from sulfur in the biomass feedstock, is mostly present as $H_2S$. Smaller amounts of e.g. mercaptanes or thiophenes are also existent. A separated process step for sulfur removal is not necessary as most of the organic sulfur compounds are hydrated in the WGS unit to become $H_2S$, which is then separated from the product gas stream in the amine scrubber. The remaining amounts of organic sulfur compounds will be separated in the PSA unit into the adsorbate. They are not problematic in the SR and do not negatively influence its performance, as the SR is operated at 850 °C. (Ashrafi, 2008) In the SR itself, sulfur is again hydrated to $H_2S$, which is then again separated in the amine scrubber. No accumulation of sulfur in the system takes place.

Mass and energy balances of the investigated hydrogen production routes were carried out using the process simulation tool COCO (CAPE-OPEN to CAPE-OPEN) is a CAPE-OPEN compliant steady-state simulation environment. (COCO simulator, 2018) Pressure losses were not considered in the calculations, and compressors were calculated with an isentropic efficiency of 75%. Heat integration was carried out, under the assumptions of a constant specific isobar heat capacity over the whole temperature range, heat losses were neglected and the minimum temperature difference was set to 20 °C. Heat of the RME scrubber was only used for the biomass dryer, excess heat of the RME scrubber was not considered, because of the low temperature level. No additional internally power or pressure recovery was considered. Tar, BTEX, and sulfur components were not taken into account in the simulation.

## Hydrogen production concept based on dual fluidized bed gasification process chain

In the following the proposed process chain for 50 MW hydrogen production, using a DFB gasification process will be addressed and discussed. Figure 35 shows the concept for hydrogen production based on the DFB gasification process and Figure 36 shows the hydrogen flows in the process. The biomass to hydrogen efficiency (LHV based) for this process is 68.9%.

In this concept the DFB gasification reactor is fed with woody biomass as feedstock and the gasification reactor is operated with steam and the combustion reactor with air. As the two reactors are separated from each other, as described in more detail above, it is not necessary to use pure oxygen as oxidizing medium. Air is sufficient for combustion as the flue gas is separately released from the DFB reactor system and therefore no dilution of $N_2$ occurs in the product gas.

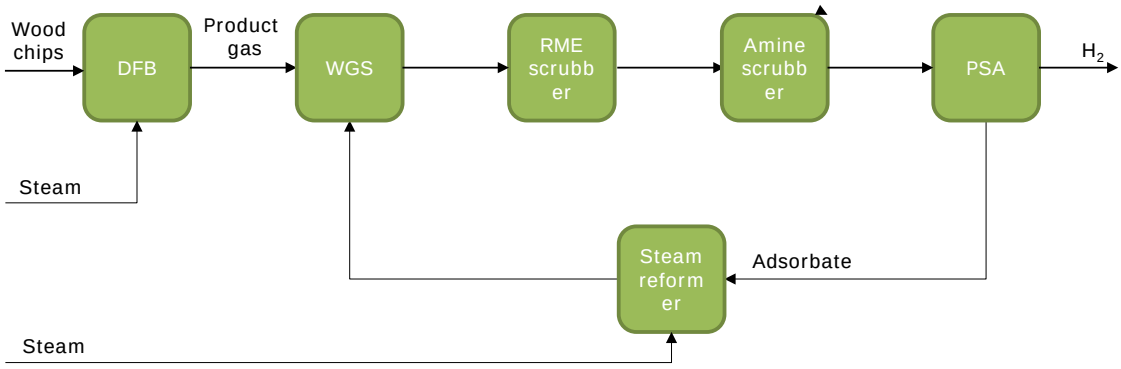


Figure 35: Simplified illustration of the investigated DFB gasification based H2 production concept.

Product gas leaving the gasification enters after cooling and filtration a WGS unit where the $H_2$ content in the product gas is further increased. Afterwards, tar is separated from the gas stream in a RME scrubber unit. In addition, a predominant portion of the steam is condensed in the RME scrubber. $CO_2$ is separated in an amine scrubber. This biomass based $CO_2$ could be utilized. However, in this study, the $CO_2$ is not considered to be utilized and therefore not considered in the techno-economic evaluation. Downstream the amine scrubber, the gas is compressed to 10 bar and fed into the PSA, where $H_2$ with high purity is separated from the remaining gas components. The adsorbate, mainly containing $CH_4$, still $H_2$, and $C_xH_y$ is fed into a SR and further recycled into the WGS unit. In addition, a part of the adsorbate is used to fire the SR.

Flue gas cleaning from the DFB combustion reactor is necessary, which typically includes cooling of the gas stream with heat exchangers and filtering for separation of fine ash. The DFB process needs a part of the energy contained in the adsorbate from the PSA internally for temperature control reasons in the combustion reactor.

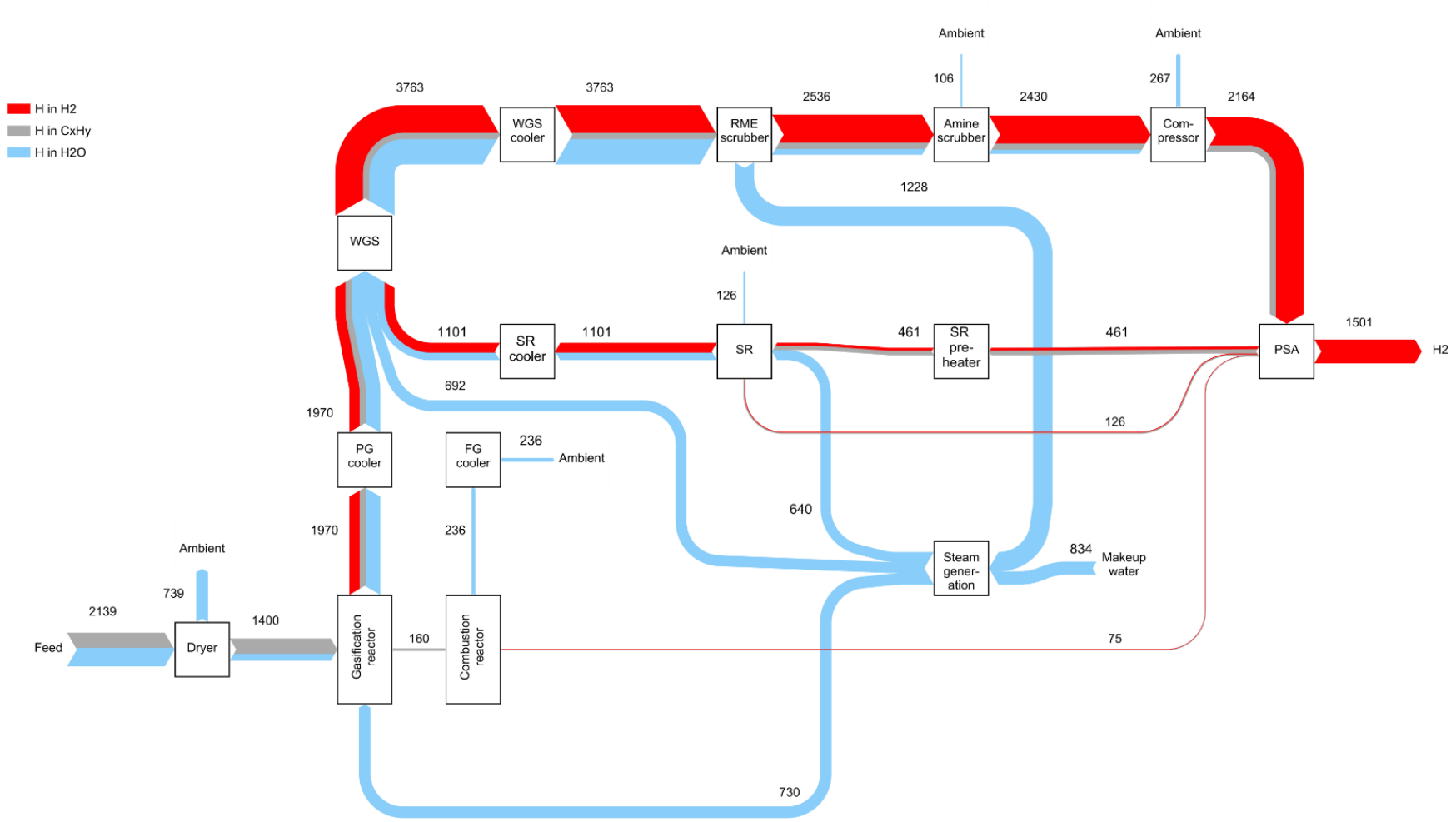


Figure 36: Sankey diagram of the investigated DFB gasification based $H_2$ production concept with 50 MW $H_2$ output showing the hydrogen flows in $H_2$, $C_xH_y$, and $H_2O$ in $kg \cdot h^{-1}$.

Table 7 shows the heat streams considered in heat integration of the DFB based concept. Figure 37 shows the resulting composite curves and the grad composite curve of the investigated DFB process. In order to maximize the hydrogen production, no product gas is burned to generate steam or heat. Instead external heat is used to meet the heat demand. Only the SR is fired with product gas. It can be seen, that in the case of 50 MW $H_2$ production, there is additional 2.6 MW heat needed.

Table 7: Heat streams of the investigated DFB gasification based $H_2$ production concept with 50 MW $H_2$ output considered for heat integration.

| Streams | T_in in °C | T_out in °C | Delta H in MW |
|---|---|---|---|
| DFB product gas cooler | 850 | 300 | 7.582 |
| DFB flue gas cooler | 930 | 150 | 15.303 |
| WGS cooler | 455 | 80 | 8.278 |
| SR cooler | 850 | 350 | 3.238 |
| SR flue gas cooler | 870 | 150 | 2.605 |
| Water pre-heater | 40 | 99 | 1.515 |
| Steam generator | 99 | 101 | 11.987 |
| Steam super-heater | 101 | 450 | 3.555 |
| SR pre-heater1 | 50 | 450 | 0.904 |
| SR pre-heater2 | 450 | 850 | 2.520 |

| Streams | T_in in °C | T_out in °C | Delta H in MW |
|---|---|---|---|
| DFB air pre-heater | 10 | 450 | 6.840 |
| Amine stripper | 110 | 120 | 12.289 |

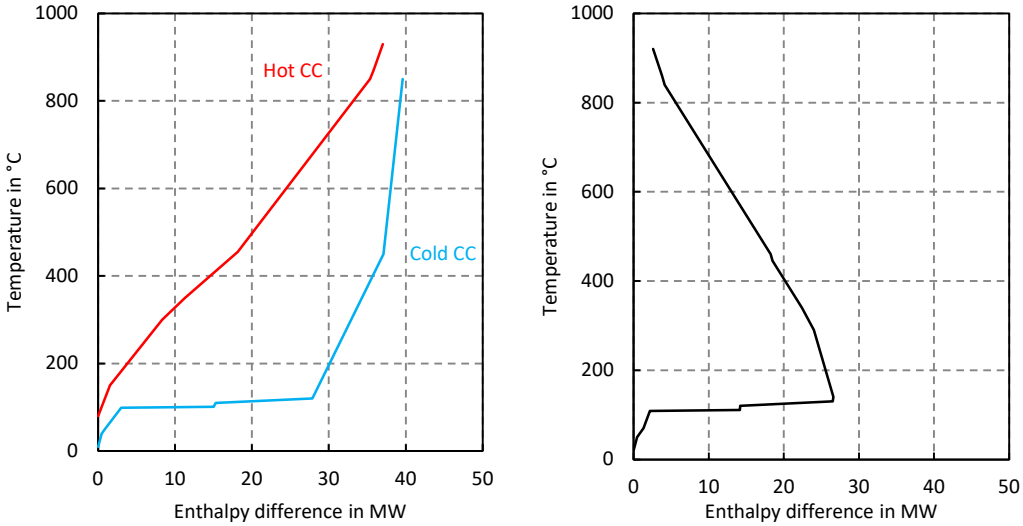


Figure 37: Composite curves (left) and grand composite curve (right) for heat streams of the investigated DFB gasification based $H_2$ production concept, with 50 MW $H_2$ output capacity.

Table 8 shows the material and energy streams which were considered for the techno-economic calculation of the DFB gasification based process chain.

Table 8: Material and energy streams of the investigated $H_2$ production process based on DFB gasification (compare (Kraussler, 2018; Müller, 2013; Yao et al., 2017))

| | | |
|---|---|---|
| H2 output capacity | 50 | MW |
| Wood chips (dry) | 15 842 | $kg \cdot h^{-1}$ |
| RME | 155 | $kg \cdot h^{-1}$ |
| Olivine | 155 | $kg \cdot h^{-1}$ |
| $CaCO_3$ | 116 | $kg \cdot h^{-1}$ |
| Makeup water | 7 458 | $kg \cdot h^{-1}$ |
| Solid disposal | 429 | $kg \cdot h^{-1}$ |

## Hydrogen production concept based on sorption enhanced reforming process chain

Figure 38 shows the concept of 1 MW hydrogen production from SER and Figure 39 shows the process more in detail, including the hydrogen flows. The SER technology is advantageous for the production of hydrogen, as the product gas is already enriched in $H_2$. On the other hand, $CO_2$ is separated from the product gas in-situ by the circulating limestone bed material, as described above. This has significant implications for the development of the process chain. As the WGS reaction is enhanced already inside the reactor, no additional WGS unit is necessary downstream from the SER reactor. Furthermore, as $CO_2$ is separated in-situ, the amine scrubber is not needed in this set-up either. Thus, the gas upgrading is achieved by only two process steps, namely the RME scrubber and the PSA unit. To simplify the process further, reforming of the hydrocarbons is skipped, with the penalty of a lower conversion to hydrogen. This process has a biomass to hydrogen efficiency (LHV based) of 33.2%.

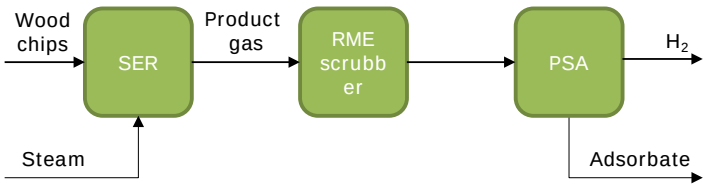


Figure 38: Simplified illustration of the investigated SER based $H_2$ production concept.

After $H_2$ with high purity is separated from the gas stream, in contrast to the DFB based process, the PSA adsorbate is not recycled. The PSA adsorbate is rich in $CH_4$ and is considered to be used as fuel gas, consequently to substitute natural gas. In the SER based process, less steam needs to be added to the system because of the absence of WGS and SR reactor. Consequently less heat is needed. However, in the SER based process, on one hand less hydrogen, but on the other hand, in addition to the hydrogen, burnable gas (PSA adsorbate) and heat is produced.

Table 9 shows the heat streams considered in heat integration of the SER based concept. Figure 40 shows the resulting composite curves and the grad composite curve of the investigated SER process. It can be seen, that in the case of 1 MW $H_2$ production, there is additional 0.1 MW heat output and 1.3 MW adsorbate output.

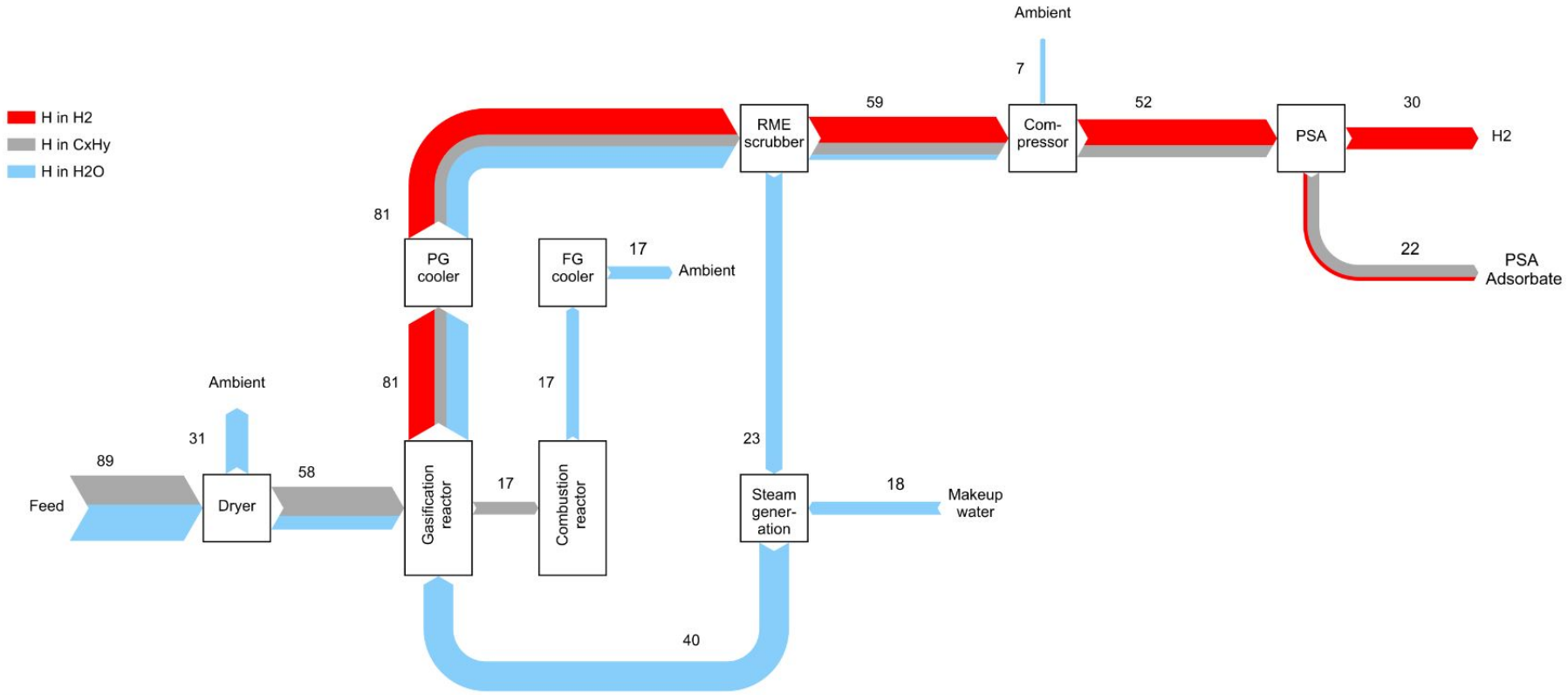


Figure 39: Sankey diagram of the investigated SER based $H_2$ production concept with 1 MW $H_2$ output showing the hydrogen flows in $H_2$, $C_xH_y$, and $H_2O$ in $kg \cdot h^{-1}$.

Table 9: Heat streams of the investigated SER gasification based $H_2$ production concept with 1 MW $H_2$ output considered for heat integration.

| Streams | T_in in °C | T_out in °C | Delta H in kW |
|---|---|---|---|
| SER product gas cooler | 675 | 80 | 253 |
| SER flue gas cooler | 900 | 150 | 635 |
| Water pre-heater | 32 | 99 | 30 |
| Steam generator | 99 | 101 | 235 |
| Steam super-heater | 101 | 450 | 70 |
| SER air pre-heater | 10 | 450 | 437 |

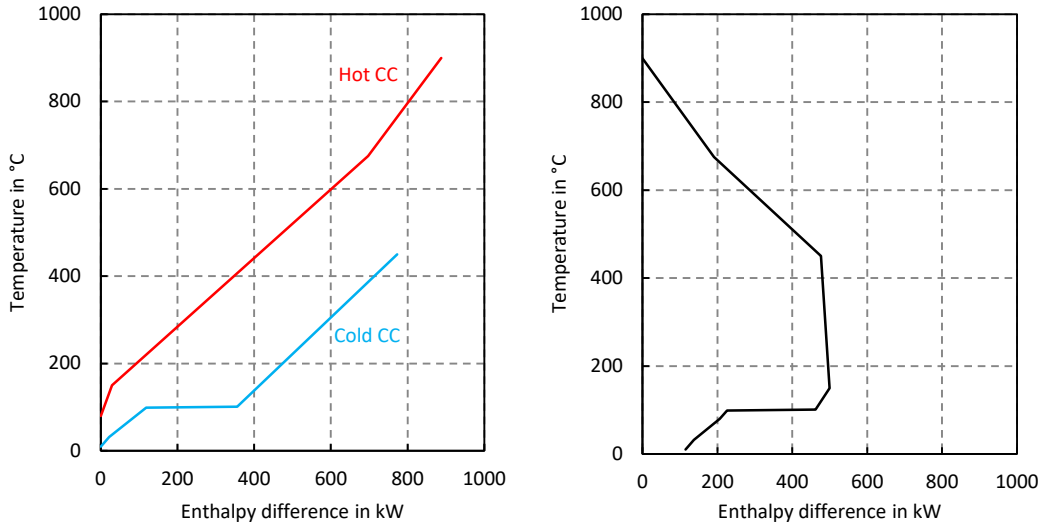


Figure 40: Composite curves (left) and grand composite curve (right) for heat steams of the investigated SER based $H_2$ production concept, with 1 MW $H_2$ output capacity.

Table 10 shows the material and energy stream which were considered for the techno-economic calculation of the SER based process chain.

Table 10: Material and energy streams of the investigated $H_2$ production process based on SER (compare (Fuchs et al., 2017; Müller, 2013))

| **$H_2$ output capacity** | **1** | **MW** |
|---|---|---|
| Wood chips (dry) | 657 | $kg \cdot h^{-1}$ |
| RME | 5 | $kg \cdot h^{-1}$ |
| $CaCO_3$ | 25 | $kg \cdot h^{-1}$ |
| Makeup water | 160 | $kg \cdot h^{-1}$ |
| Solid disposal | 31 | $kg \cdot h^{-1}$ |
| Heat (generated) | 115 | kW |
| PSA adsorbate (generated) | 1 349 | kW (LHV based) |

Summarizing, two process chains for the production of hydrogen were presented in detail and discussed. However, it needs to be noted at this point, that other production routes may be found suitable. At this stage, the development of such technologies is still at its beginning. Other concept might be suitable as well based on other separation steps, such as membranes. These production routes were chosen exemplary based on the aim to simplify the process chains to a minimum of upgrading steps. Thus, the WGS unit, the RME and amine scrubbers, the PSA, and the SR were included in the processes when applicable. Membranes were not included into the development of the process chains as the additional effort was assessed to be too high, as an additional compression step needs to be included into the process chain. This is due to the fact that the product gas needs to be compressed before the membrane and $H_2$ is present as permeate (depressurized) after the membrane, which needs to be compressed again before entering a PSA.

The two described hydrogen production routes, based on the gasification of biomass, will be further investigated in a techno-economic assessment.

## Technology readiness level assessment

This chapter will give an overview of the assessment of the Technology Readiness Levels (TRL) of the single components and the complete process chains. Figure 41 shows the basic concept of the TRL assessment. It will be discussed, that even though the single unit operations needed for the complete process chains can be evaluated with comparably high TRL levels, the complete process chains need to be assessed with significantly lower TRL levels. This is due to the fact, that even though most of the unit operations are proven technologies, the complete process chains have not yet been demonstrated in commercial scale. Thus, considering the additional complexity to the assessment, the overall TRLs are chosen accordingly. Nevertheless, as the process chains have been developed based on the fact, that the single operation units are technologically proven processes, the further development of the process chains can be considered as advantageous compared to less developed technologies.

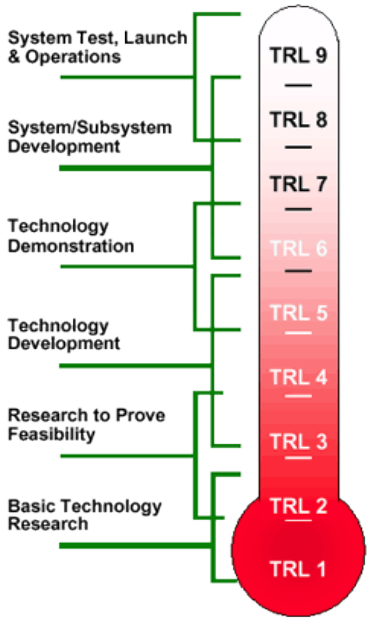


Figure 41: Illustration of the concept of the technology readiness level (TRL).

### Single components

First, the single components, which are considered in the process chains, will be assessed regarding their TRL level. Here, it is not considered if the single components have been integrated and established to work together. Thus, the assessment is only valid for the components themselves. Table 11 shows the TRLs of the single components.

Table 11: TRL levels of the single components used in the investigated process chains.

| Component | TRL | Additional comments, when TRL is lower than 9 |
|---|---|---|
| DFB | 8 | The DFB process has reached market maturity and is operated commercially in e.g. Senden, near Ulm, Germany. However, due to the fact that maximum annual operation hours of about 7 500 is only reached (goal: 8 000 $h \cdot a^{-1}$), the TRL level is not set to 9. |
| SER | 5 | The SER process is similar to the DFB process regarding the reactor concept, which adds certain security to the development. Pilot-scale experiments have shown successful operation, however no demonstration plant is yet available. TRL 6 would require experimental experience near the desired configuration in terms of performance, weight, and volume. The operated pilot-scale test-rigs are larger in capacity than simple laboratory test-rigs, but are still smaller than the desired capacity. |
| WGS | 9 | Commercially available from several suppliers |
| RME Scrubber | 8 | The RME scrubber has been successfully used in commercial DFB plants and has been technologically proven. The TRL assessment is equivalent to that of the DFB process, which results in a value of 8. |
| Amine Scrubber | 9 | Commercially available from several suppliers |
| PSA | 9 | Commercially available from several suppliers |
| Steam reformer | 9 | Commercially available from several suppliers |
| Flue gas cleaning | 9 | Commercially available from several suppliers |

### Complete process chains

Based on the assessment of the single components, in the following the complete process chains will be evaluated regarding the TRL levels. Here, the assessment is based on the availability of the integrated system, thus meaning, that the single components are evaluated regarding the technological and experimental proof, if they work together successfully. As described above, it is however necessary to consider the further development of the process chain based on the single components. The further development might result in a faster increase of the TRL levels of the process chains than it would be expected for new technologies based on non-proven operation units. Thus, often published assumptions on the years necessary for reaching the market maturity are not necessarily applicable here. Table 12 shows the TRLs of the process chains.

Table 12: TRL levels of the total process chains investigated.

| Process chain | TRL | Additional comments |
|---|---|---|
| Process chain based on DFB | 5 | The complete system has been tested with other supporting elements in a simulated operational environment with real product gas from a commercial DFB plant. The full process chain has been proven to work in laboratory-scale (single components have been established to work together). The process chain has not yet been tested near the desired configuration in terms of performance, weight, and volume. |
| Process chain based on SER | 3 | Laboratory tests have been performed; analytical predictions are available; according fidelity of experimental experience of full process chain under desired conditions is not yet established. |

Experimental investigations have been performed for different biogenic feedstock and published results are available, as described above. Furthermore, the development of the above described process chains is on-going and new results are expected in the near future.

# Techno-economic assessment

This section presents the methodology and the results of the techno-economic assessment. Mixed financing is not considered, so the total investment is taken by the company. Plant life-time and depreciation-time were chosen to be the same.

## METHODOLOGY

The techno-economic assessment is based on previously developed approaches, and the simple straight-line method was applied, compare (Brown, 2007). Based on the above mentioned routes and comparison with other state of the art $H_2$ production routes, this section describes the methodology used for the techno-economic assessment.

Capital expenditures (CAPEX) were estimated based on a literature study as well as on budget quotes from different plant manufacturers. Investment costs from years other than 2016 were adjusted using the chemical engineering plant cost index (CEPI, see Equation 18).

$$\frac{\text{CAPEX 1}}{\text{CAPEX 2}} = \frac{\text{CEPI 1}}{\text{CEPI 2}} \qquad \text{Equation 18}$$

In order to calculate the CAPEX of the plants capacities, Equation 19 was used.

$$\frac{\text{CAPEX 1}}{\text{CAPEX 2}} = \left(\frac{\text{Capacity 1}}{\text{Capacity 2}}\right)^{\text{m}} \qquad \text{Equation 19}$$

An exponent m of 0.67 was used as scaling factor for the plants. In addition, plant start-up expenses (SUEX) were considered to be 10% of the calculated CAPEX. Therefore, the overall investment costs (INV) of a plant were calculated according to Equation 20.

$$\text{INV} = \text{CAPEX} + \text{SUEX} \qquad \text{Equation 20}$$

Table 13 and Table 14 show the specific costs and prices of the different considered material and energy streams as well as estimates for the calculation of the operating expenses (OPEX).

Table 13: Specific costs and prices of the investigated material and energy streams. (compare (Kraussler, 2018; Müller, 2013; Yao et al., 2017))

| | | Values | Units |
|---|---|---|---|
| Raw material | Wood chips (dry) | 0.091 | EUR·kg$^{-1}$ |
| Utilities | Electricity | 0.080 | EUR·kWh$^{-1}$ |
| | Heat | 0.050 | EUR·kWh$^{-1}$ |
| | RME | 1.100 | EUR·kg$^{-1}$ |
| | $CaCO_3$ | 0.150 | EUR·kg$^{-1}$ |
| | Olivine | 0.156 | EUR·kg$^{-1}$ |
| | Silica sand | 0.060 | EUR·kg$^{-1}$ |
| | Solid disposal | 0.090 | EUR·kg$^{-1}$ |
| | Make-up water | 0.002 | EUR·kg$^{-1}$ |

In the SER case, there are to more output streams in addition to the hydrogen: heat and the PSA adsorbate. The heat generated is priced as well as the heat needed with 0.05 EUR·kWh$^{-1}$. The PSA adsorbate is used to substitute natural gas. This is calculated on the LHV. The price for the PSA adsorbate was calculated by using the natural gas price (34.51 EUR·MWh$^{-1}$, compare ("E-Control," 2018)) and the price for $CO_2$ emission (20.27 EUR·tCO2$^{-1}$, compare ("European Emission Allowances," 2018)).

Table 14: Detailed and factored estimates for the calculation of the OPEXs.

<table>
<tr><th></th><th colspan="2">Detailed estimate</th><th>Factored estimate</th></tr>
<tr><td rowspan="2">Raw material and utilities</td><td>DFB:</td><td>See Table 8, compare (Kraussler, 2018; Yao et al., 2017)</td><td rowspan="2"></td></tr>
<tr><td>SER:</td><td>See Table 10, compare (Fuchs et al., 2017; Müller, 2013)</td></tr>
<tr><td>Operating labor</td><td colspan="2">See Table 15: Assumptions for the techno-economic assessment.</td><td></td></tr>
<tr><td>Maintenance, insurance and taxes</td><td colspan="2"></td><td>5% of CAPEX</td></tr>
</table>

The depreciation was calculated according to Equation 21.

$$\text{Depreciation} = \frac{\text{INV}}{\text{n}} \qquad \text{Equation 21}$$

Table 15 shows the assumptions for the techno-economic assessment covering the number of operators, their wage, the annual operating time, the overall plant lifetime, and the chosen return on investment (ROI). It was assumed that the plants need between 1 (1 MW) and 12 (50 MW), operators in order to ensure a safe and reliable twenty-four-seven operation. In addition, a tax rate of 25% and a return of investment of 10% was chosen.

Table 15: Assumptions for the techno-economic assessment.

| | Values | Units |
|---|---|---|
| Operators | 1 (1 MW)<br>12 (50 MW) | - |
| Wage per operator | 75 000 | EUR·a$^{-1}$ |
| Annual operating time (t) | 8000 | h·a$^{-1}$ |
| Plant lifetime (n) | 20 | a |
| Tax rate | 25% | - |
| Return on investment (ROI, i) | 10% | - |

The annual revenues (REV) were calculated according to Equation 22. The DFB process, based only on the hydrogen production. The SER process based on hydrogen, heat, and PSA adsorbate production. Further, possible side products (e.g. $CO_2$) generated, were not taken into account.

$$\mathrm{REV} = \dot{m}_{H_2} \cdot t \cdot \text{hydrogen selling price} + (\text{heat} \cdot M \cdot \text{heat selling price} + \text{PSA adsorbate} \cdot t \cdot \text{PSA adsorbate selling price}) \quad \text{Equation 22}$$

The before tax (BT) cash flow was calculated according to Equation 23 as the difference of annual revenues (REV) and annual OPEX.

$$\text{BT cash flow} = \mathrm{REV} - \mathrm{OPEX} - \text{Depreciation} \quad \text{Equation 23}$$

The after tax (AT) cash flow was calculated according to Equation 24 which takes the BT cash flow and the tax rate into account.

$$\text{AT cash flow} = \text{BT cash flow} \cdot (1 - \text{Tax rate}) + \text{Depreciation} \quad \text{Equation 24}$$

The techno-economic assessments were based on the net present value (NPV), which was calculated with the AT cash flow, the discount rate, the plant lifetime, and the investment costs according to Equation 25.

$$\mathrm{NPV} = \mathrm{AT\ cash\ flow}\left(\frac{(1+\mathrm{i})^{\mathrm{n}}-1}{\mathrm{i}\cdot(1+\mathrm{i})^{\mathrm{n}}}\right) - \mathrm{INV} \qquad \text{Equation 25}$$

Based on the assumption NPV = 0, the specific selling price of the produced $H_2$ was calculated.

In addition, the following key figures were calculated to describe the techno-economics of the investigated processes.

The specific INV were calculated according to Equation 26.

$$\mathrm{INV_s} = \frac{\mathrm{INV}}{\dot{m}_{\mathrm{H_2}}\cdot \mathrm{LHV}\cdot \mathrm{n}\cdot \mathrm{t}} \qquad \text{Equation 26}$$

The specific OPEX were calculated according to Equation 27.

$$\mathrm{OPEX_s} = \frac{\mathrm{OPEX}}{\dot{m}_{\mathrm{H_2}}\cdot \mathrm{LHV}\cdot \mathrm{t}} \qquad \text{Equation 27}$$

The specific total expenditures ($TOTEX_s$) are the sum of INVs and OPEXs, see Equation 28.

$$\mathrm{TOTEX_s} = \mathrm{INV_s} + \mathrm{OPEX_s} \qquad \text{Equation 28}$$

The following presents the data used for the techno-economic evaluation of the three investigated hydrogen production routes.

## RESULTS AND DISCUSSION

This section presents the results of the techno-economic assessment. Two different $H_2$ production routes, a DFB based 50 MW $H_2$ production capacity process and a SER based 1 MW $H_2$ production capacity process. Each based on gasification of biomass, are presented.

### Hydrogen production based on dual fluidized bed gasification

Table 16 summarizes the results of the techno-economic assessment, based on the DFB gasification based route. The $H_2$ selling price and thereby the REV was calculated on the assumption NPV = 0, compare (Kraussler, 2018; Müller, 2013; Yao et al., 2017).

Table 16: Results of the techno-economic assessment of the $H_2$ production process based on DFB gasification.

| $H_2$ output capacity | 50 | MW |
|---|---|---|
| INV | 64 900 000 | EUR |
| OPEX | 23 379 000 | $EUR \cdot a^{-1}$ |
| REV | 32 461 000 | $EUR \cdot a^{-1}$ |
| $H_2$ selling price for NPV = 0 | 2.70 | $EUR \cdot kg^{-1}$ |

Figure 42 illustrates the annual costs for raw material and utilities for the 50 MW $H_2$ output. It can be seen, that the costs for the wood chips and the costs for electricity represent the main share of annual raw material and utility costs.

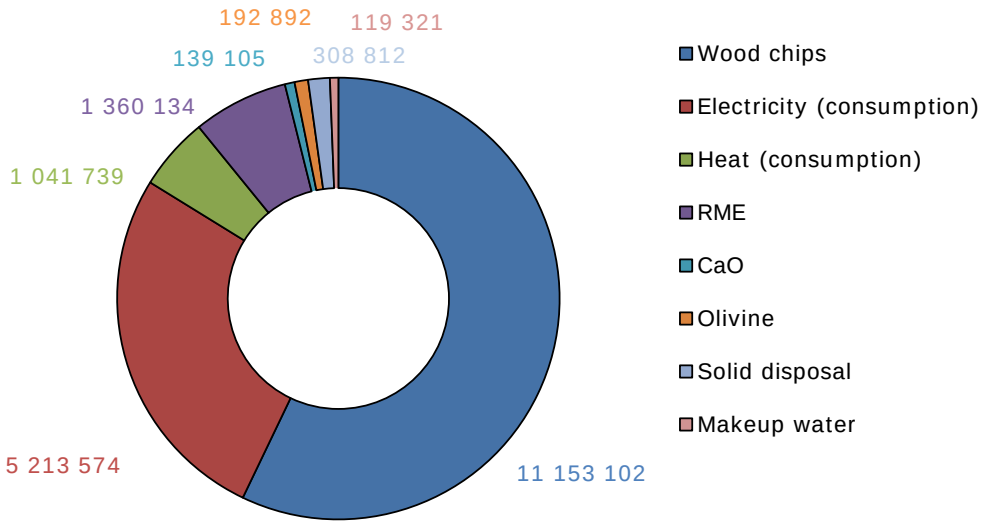


Figure 42: Distribution of annual raw material and utility costs based on the DFB 50 MW plant in EUR·a$^{-1}$.

## Hydrogen production based on sorption enhanced reforming process

Table 17 summarizes the results of the techno-economic assessment, based on the SER route. SER based routes show lower INV costs for downstream gas upgrading, on the other hand a larger SER process itself is needed, caused by the lower hydrogen yield, because of no gas recycling. On the other hand heat and the PSA adsorbate are utilized as product streams, compare (Müller, 2013; Yao et al., 2017)).

Table 17: Results of the techno-economic assessment of the $H_2$ production process based on SER.

| $H_2$ output capacity | 1 | MW |
|---|---|---|
| INV | 5 500 000 | EUR |
| OPEX | 1 009 000 | EUR·a$^{-1}$ |
| REV | 1 779 000 | EUR·a$^{-1}$ |
| $H_2$ selling price for NPV = 0 | 5.49 | EUR·kg$^{-1}$ |

Figure 43 illustrates the annual costs for raw material and utilities for the 1 MW $H_2$ output. In the case of the SER based route, the share of costs for bed material and solid disposal becomes more. Compared to DFB gasification, caused by the soft bed material used and therefore higher abrasion

rates. Figure 45 illustrates the distributions of the annual revenues, based on the three products: hydrogen, PSA adsorbate, and heat.

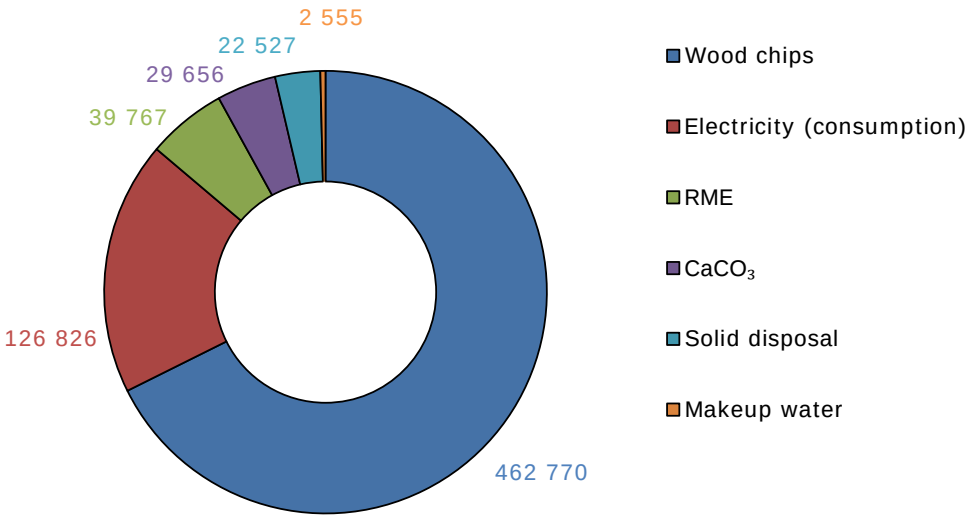


Figure 43: Distribution of annual raw material and utility costs based on the 1 MW SER plant in EUR·a$^{-1}$.

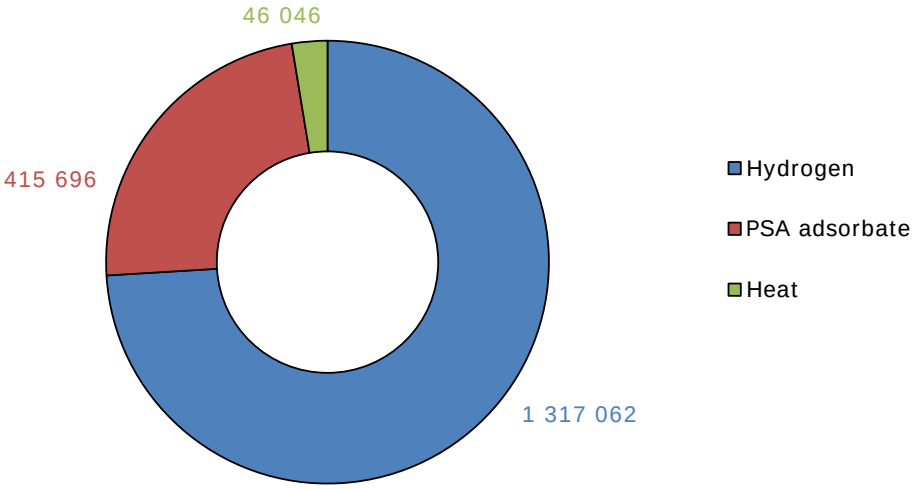


Figure 44: Distribution of annual revenues based on the 1 MW SER plant in EUR·a$^{-1}$.

## Comparison of results

Table 18 shows the comparison in terms of H2 selling price of the investigated hydrogen production routes. Figure 45 summarizes the TOTEXs of the produced H2 over the production capacity and process chain applied. Selling price and production costs via biomass gasification are higher, but in the same price range, compared to state of the art fossil based hydrogen production. (Mueller-Langer et al., 2007) reports production costs of natural gas steam reforming plants between 1.03 EUR·kg-1 (large scale) and 2.60 EUR·kg-1 (small scale). Those comparably low production costs can be, on the one hand, dedicated to the low natural gas price and, on the other hand, to the high efficiency of natural gas steam reforming plants.

Table 18: Comparison of the calculated hydrogen selling price, based on the assumption NPV = 0.

| Hydrogen production capacity | SER 1 MW | DFB 50 MW |
|---|---|---|
| Hydrogen selling price in EUR·kg$^{-1}$ | 5.49 | 2.70 |

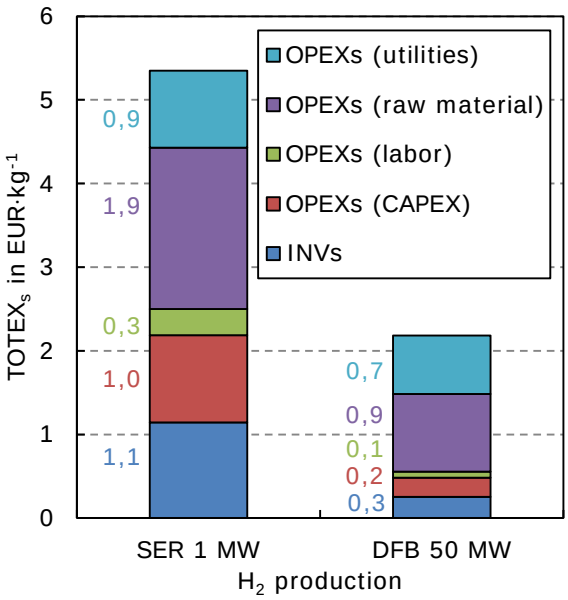


Figure 45: Comparison of the calculated TOTEXs based on the three different H2 production chains and on the three different H2 production capacities.

# Conclusion and outlook

This study on the production of hydrogen via biomass gasification, different possible technological routes were discussed and compared. Based on available knowledge from research and development of hydrogen production via gasification, a small and medium scale process chain was derived and further evaluated. The evaluation was based on the development of the process chains regarding the single operation units, an assessment of the TRL and techno-economic evaluation.

Overall it can be stated, that for implementation of biomass gasification-based hydrogen production governmental support and subsidies are necessary. Especially in the first 15 years of the development towards market maturity and stable operation and production, political support is necessary. Today, framework conditions are yet missing for biomass gasification-based hydrogen production to be economically competitive to fossil-based hydrogen production. Technology roadmaps and political goals (e.g. in the United States of America and the EU 4) include hydrogen production via biomass gasification in the future with a significant increase of the capacity until 2050.

Currently, promising process chains have not yet been tested in demonstration scale near the desired configuration in terms of performance, weight, and volume. However, the discussed process chains are based on the utilization on developed and technologically proven operation units (TRLs of 8 and above for DFB gasification, gas cleaning and upgrading) and therefore, the development of the process chains to market maturity could be achieved in the near future. Consequently research and development is needed in order to establish demonstration of the full process chain for the implementation of the technology.

As gas upgrading unit operations, such as WGS, scrubbers and PSA units, are technologically proven and available on the market, gasification technologies and their integration with established gas upgrading unit operations are still the bottleneck regarding the market maturity of the overall process. Furthermore, the feedstock spectrum has to be broadened in the future to increase the flexibility of the process and improve the overall economic feasibility.

# Annex

Data tables of the simulation, which were carried out to acquire the mass and energy balance if the investigated routes.

DFB route with 50 MW $H_2$ capacity:

| Stream | DFB product gas | WGS steam | WGS inlet | WGS outlet |
|---|---|---|---|---|
| Pressure in bar | 1 | 1 | 1 | 1 |
| Temperature in °C | 850 | 450 | 337 | 448 |
| Mole frac Hydrogen | 0.2609 | 0.0000 | 0.2789 | 0.3846 |
| Mole frac Carbon monoxide | 0.1426 | 0.0000 | 0.1323 | 0.0265 |
| Mole frac Carbon dioxide | 0.1446 | 0.0000 | 0.0802 | 0.1860 |
| Mole frac Methane | 0.0622 | 0.0000 | 0.0340 | 0.0340 |
| Mole frac Ethylene | 0.0146 | 0.0000 | 0.0080 | 0.0080 |
| Mole frac Ethane | 0.0018 | 0.0000 | 0.0010 | 0.0010 |
| Mole frac Nitrogen | 0.0064 | 0.0000 | 0.0115 | 0.0115 |
| Mole frac Water | 0.3669 | 1.0000 | 0.4543 | 0.3485 |
| Flow rate in kg · $h^{-1}$ | 23766 | 6183 | 38930 | 38930 |

| Stream | RME scrubber inlet | Amine scrubber inlet | PSA inlet | H2 (PSA raffinate) |
|---|---|---|---|---|
| Pressure in bar | 1 | 1 | 10 | 10 |
| Temperature in °C | 100 | 50 | 50 | 50 |
| Mole frac Hydrogen | 0.3846 | 0.5251 | 0.8229 | >0.9997 |
| Mole frac Carbon monoxide | 0.0265 | 0.0362 | 0.0567 | <0.0001 |
| Mole frac Carbon dioxide | 0.1860 | 0.2538 | 0.0040 | <0.0001 |
| Mole frac Methane | 0.0340 | 0.0464 | 0.0727 | <0.0001 |
| Mole frac Ethylene | 0.0080 | 0.0109 | 0.0170 | <0.0001 |
| Mole frac Ethane | 0.0010 | 0.0013 | 0.0021 | <0.0001 |
| Mole frac Nitrogen | 0.0115 | 0.0157 | 0.0246 | <0.0001 |
| Mole frac Water | 0.3485 | 0.1107 | 0.0000 | <0.0001 |
| Flow rate in kg · $h^{-1}$ | 38930 | 27963 | 6191 | 1501 |

| Stream | PSA adsorbate | Recycle to DFB | Heating SR | SR steam |
|---|---|---|---|---|
| Pressure in bar | 1 | 1 | 1 | 1 |
| Temperature in °C | 48 | 48 | 48 | 450 |
| Mole frac Hydrogen | 0.4108 | 0.4108 | 0.4108 | 0.0000 |
| Mole frac Carbon monoxide | 0.1888 | 0.1888 | 0.1888 | 0.0000 |
| Mole frac Carbon dioxide | 0.0132 | 0.0132 | 0.0132 | 0.0000 |
| Mole frac Methane | 0.2418 | 0.2418 | 0.2418 | 0.0000 |
| Mole frac Ethylene | 0.0567 | 0.0567 | 0.0567 | 0.0000 |
| Mole frac Ethane | 0.0070 | 0.0070 | 0.0070 | 0.0000 |

| | | | | |
|---|---|---|---|---|
| Mole frac Nitrogen | 0.0817 | 0.0817 | 0.0817 | 0.0000 |
| Mole frac Water | 0.0000 | 0.0000 | 0.0000 | 1.0000 |
| Flow rate in kg · $h^{-1}$ | 4690 | 533 | 893 | 5719 |

| Stream | SR inlet | SR outlet | Steam gasifier |
|---|---|---|---|
| Pressure in bar | 1 | 1 | 1 |
| Temperature in °C | 850 | 850 | 450 |
| Mole frac Hydrogen | 0.1693 | 0.4495 | 0.0000 |
| Mole frac Carbon monoxide | 0.0778 | 0.1794 | 0.0000 |
| Mole frac Carbon dioxide | 0.0055 | 0.0043 | 0.0000 |
| Mole frac Methane | 0.0996 | 0.0898 | 0.0000 |
| Mole frac Ethylene | 0.0234 | 0.0000 | 0.0000 |
| Mole frac Ethane | 0.0029 | 0.0000 | 0.0000 |
| Mole frac Nitrogen | 0.0337 | 0.0263 | 0.0000 |
| Mole frac Water | 0.5880 | 0.3404 | 1.0000 |
| Flow rate in kg · $h^{-1}$ | 8981 | 8981 | 5641 |

SER route with 1 MW $H_2$ capacity:

| Stream | SER product gas | PSA inlet | H2 (PSA raffinate) | PSA adsorbate | Steam gasifier |
|---|---|---|---|---|---|
| Pressure in bar | 1 | 10 | 10 | 1 | 1 |
| Temperature in °C | 675 | 50 | 50 | 47 | 450 |
| Mole frac Hydrogen | 0.4154 | 0.6359 | >0.9997 | 0.2076 | 0.0000 |
| Mole frac Carbon monoxide | 0.0596 | 0.0912 | <0.0001 | 0.1986 | 0.0000 |
| Mole frac Carbon dioxide | 0.0740 | 0.1133 | <0.0001 | 0.2466 | 0.0000 |
| Mole frac Methane | 0.0780 | 0.1194 | <0.0001 | 0.2599 | 0.0000 |
| Mole frac Ethylene | 0.0085 | 0.0130 | <0.0001 | 0.0283 | 0.0000 |
| Mole frac Ethane | 0.0066 | 0.0101 | <0.0001 | 0.0220 | 0.0000 |
| Mole frac Nitrogen | 0.0111 | 0.0170 | <0.0001 | 0.0370 | 0.0000 |
| Mole frac Water | 0.3468 | 0.0000 | <0.0001 | 0.0000 | 1.0000 |
| Flow rate in kg·$h^{-1}$ | 591 | 327 | 30 | 297 | 361 |

# List of Figures

# List of Tables

# Nomenclature

## ABBREVIATION AND ACRONYMS

| | |
|---|---|
| aMDEA | Activated Methyldiethanolamine |
| ASU | Air separation unit |
| ATR | Autothermal reforming |
| AUT | Austria |
| BFB | Bubbling fluidized bed |
| BioSNG | Biomass derived synthetic natural gas |
| BTEX | Benzene, toluene, ethylbenzene, and xylenes |
| CCS | Carbon capture and sequestration |
| CHP | Combined heat and power |
| CPO | Catalytic partial oxidation |
| DEU | Germany |
| DEA | Diethanolamine |
| DFB | Dual fluidized bed |
| DME | Dimethyl ether |
| ECN | Energy Research Centre of the Netherlands |
| EF | Entrained flow |
| ESP | Electrostatic precipitators |
| EU | European Union |
| EU 4 | Germany, Scandinavia, France, and UK |
| FRA | France |
| FT | Fischer-Tropsch |
| GCMS | Gas chromatograph coupled with a mass spectrometer |
| HT | High temperature |
| INV | Investment costs |
| ITA | Italy |
| LT | Low temperature |
| MCFC | Molten carbonate fuel cell |
| MDEA | Methyldiethanolamine |

| | |
|---|---|
| MDI | Methylene-diphenyl-diisocyanate |
| MEA | Monoethanolamine |
| NG | Natural gas |
| ORC | Organic rankine cycle |
| PEM | Proton exchange membrane |
| PEMFC | Proton exchange membrane fuel cell |
| POX | Noncatalytic partial oxidation |
| PSA | Pressure swing adsorption |
| PROX | Preferential oxidation |
| PZ | Piperazine |
| RED | Renewable energy directive according to the European Union |
| ROI | Return of invest |
| SCR | Selective catalytic reduction |
| SER | Sorption enhanced reforming |
| SR | Steam reforming |
| SNG | Synthetic natural gas |
| SOFC | Solid oxide fuel cell |
| SWE | Sweden |
| TDI | Toluene-diisocyanate |
| THA | Thailand |
| TRL | Technology readiness level |
| RME | Rapeseed oil methyl ester |
| UNFCCC | United Nations Framework Convention on Climate Change |
| USA | United States |
| WEP | Wet electrostatic precipitators |
| WGS | Water gas shift |

## SYMBOLS

| | |
|---|---|
| AT cash flow | After tax cash flow in $EUR \cdot a^{-1}$ |
| BT cash flow | Before tax cash flow in $EUR \cdot a^{-1}$ |
| Capacity | NG substitute plant capacity in MW |
| CAPEX | Capital expenditures in EUR |
| INV | Investment costs considering CAPEX and SUEX in EUR |
| INVs | Specific investment costs in $EUR\ MWh^{-1}$ |
| LHV | Lower heating value in $MJ \cdot kg^{-1}$ |
| $\dot{m}_i$ | Mass flow of component in $kg \cdot s^{-1}$ |
| n | Plant lifetime in a |
| NPV | Net present value in EUR |
| OPEX | Operating expenditures in $EUR \cdot a^{-1}$ |
| OPEXs | Specific OPEX in $EUR \cdot MWh^{-1}$ |
| Revenues | Revenues generated from the selling of natural gas substitute in $EUR \cdot a^{-1}$ |
| i | Return of investment in - |
| SUEX | Start-up expenses in EUR |
| t | Annual operating time in $h \cdot a^{-1}$ |
| TOTEXs | Specific total expenditures in $EUR \cdot MWh^{-1}$ |

# Bibliography


Andersson, K.J., Skov-Skjøth Rasmussen, M., Højlund Nielsen, P.E., 2017. Industrial-scale gas conditioning including Topsoe tar reforming and purification downstream biomass gasifiers: An overview and recent examples. Fuel 203, 1026–1030. https://doi.org/10.1016/j.fuel.2017.02.085

Arregi, A., Amutio, M., Lopez, G., Bilbao, J., Olazar, M., 2018. Evaluation of thermochemical routes for hydrogen production from biomass: A review. Energy Convers. Manag. 165, 696–719. https://doi.org/10.1016/j.enconman.2018.03.089

Ashrafi, M., 20008. Hydrogen-Rich Gas Production hrough Steam Reforming of Biogas: Experimental Study and Modelling (PhD Thesis). TU Wien, Wien.

Bailey, D.W., Feron, P.H.M., 2005. Post-combustion Decarbonisation Processes. Oil Gas Sci. Technol. 60, 461–474.

Balat, H., Kırtay, E., 2010. Hydrogen from biomass – Present scenario and future prospects. Int. J. Hydrog. Energy 35, 7416–7426. https://doi.org/10.1016/j.ijhydene.2010.04.137

Ball, M., Wietschel, M., 2009. The future of hydrogen – opportunities and challenges☆. Int. J. Hydrog. Energy 34, 615–627. https://doi.org/10.1016/j.ijhydene.2008.11.014

Bardolf, R., 2017. Optimierung eines Produktgaswäschers bei der Biomassedampfvergasung im Zweibettwirbelschichtverfahren (PhD thesis). TU Wien, Vienna.

Bauer, F., Persson, T., Hulteberg, C., Tamm, D., 2013. Biogas upgrading - technology overview, comparison and perspectives for the future. Biofuels Bioprod. Biorefining 7, 499–511. https://doi.org/10.1002/bbb.1423

Brown, T., 2007. Engineering economics and economic design for process engineers. CRC Press, Boca Raton.

Chaubey, R., Sahu, S., James, O.O., Maity, S., 2013. A review on development of industrial processes and emerging techniques for production of hydrogen from renewable and sustainable sources. Renew. Sustain. Energy Rev. 23, 443–462. https://doi.org/10.1016/j.rser.2013.02.019

Chianese, S., Fail, S., Binder, M., Rauch, R., Hofbauer, H., Molino, A., Blasi, A., Musmarra, D., 2016. Experimental investigations of hydrogen production from CO catalytic conversion of tar rich syngas by biomass gasification. Catal. Today 277, 182–191. https://doi.org/10.1016/j.cattod.2016.04.005

Chianese, S., Loipersböck, J., Malits, M., Rauch, R., Hofbauer, H., Molino, A., Musmarra, D., 2015. Hydrogen from the high temperature water gas shift reaction with an industrial Fe/Cr catalyst using biomass gasification tar rich synthesis gas. Fuel Process. Technol. 132, 39–48. https://doi.org/10.1016/j.fuproc.2014.12.034

COCO simulator, 2018. COCO - the CAPE-OPEN to CAPE-OPEN simulator [WWW Document]. URL https://www.cocosimulator.org/ (accessed 3.9.18).

Corella, J., Toledo, J.M., Molina, G., 2007. A Review on Dual Fluidized-Bed Biomass Gasifiers. Ind. Eng. Chem. Res. 46, 6831–6839. https://doi.org/10.1021/ie0705507

Díaz Pérez, N.F., 2013. Hydrogen separation from producer gas generated by biomass steam gasification (PhD thesis). TU Wien, Vienna.

Düker, A., 2011. Hydrogen Production and Application in Industry. In Presentation Süd - Chemie AG.

Dunn, S., 2002. Hydrogen futures: toward a sustainable energy system. Int. J. Hydrog. Energy 27, 235–264. https://doi.org/10.1016/S0360-3199(01)00131-8

E-Control [WWW Document], 2018. URL https://www.e-control.at/gewerbe-gaspreis-monitor

European Emission Allowances [WWW Document], 2018. URL https://www.eex.com/en/market-data/environmental-markets/spot-market/european-emission-allowances#!/2018/11/12

Fail, S., 2014. Biohydrogen Production Based on the Catalyzed Water Gas Shift Reaction in Wood Gas (PhD Thesis). TU Wien.

Fail, S., Diaz, N., Benedikt, F., Kraussler, M., Hinteregger, J., Bosch, K., Hackel, M., Rauch, R., Hofbauer, H., 2014. Wood Gas Processing To Generate Pure Hydrogen Suitable for

PEM Fuel Cells. ACS Sustain. Chem. Eng. 2, 2690–2698. https://doi.org/10.1021/sc500436m
Fraile, D., Lanoix, J.-C., Maio, P., Rangel, A., Torres, A., 2015. Overview of the market segmentation for hydrogen across potential customer groups, based on key application areas. CertifHy.
Fuchs, J., Schmid, J., Müller, S., Benedikt, F., Hammerschmied, M., Kieberger, N., Stocker, H., Hofbauer, H., Bürgler, T., 2017. ERBA II - Optimierung von „Sorption Enhanced Reforming“ zur Verbesserung der CO2-Bilanz in der Roheisenerzeugung mittels Biomasse (Publizierbarer Endbericht).
Gahleitner, G., 2013. Hydrogen from renewable electricity: An international review of power-to-gas pilot plants for stationary applications. Int. J. Hydrog. Energy 38, 2039–2061. https://doi.org/10.1016/j.ijhydene.2012.12.010
GTI, 2015. Green Gasoline from Wood using Carbona Gasification and Topsoe TIGAS Process, Final Report (No. DE-EE0002874).
Hawthorne, C., Poboss, N., Dieter, H., Gredinger, A., Zieba, M., Scheffknecht, G., 2012. Operation and results of a 200-kWth dual fluidized bed pilot plant gasifier with adsorption-enhanced reforming. Biomass Convers. Biorefinery 2, 217–227. https://doi.org/10.1007/s13399-012-0053-3
Hefner III, R.A., 2002. The age of energy gases. Int. J. Hydrog. Energy 27, 1–9. https://doi.org/10.1016/S0360-3199(01)00079-9
Hofbauer, H., Rauch, R., Bosch, K., Aichernig, C., 2002. Biomass CHP Plant Güssing - A Success Story. Pyrolysis Gasif. Biomass Waste.
Insenstadt, A., Lutsey, N., 2017. Developing hydrogen fueling infrastructure for fuel cell vehicles: A status update. icct - The international council on clean transportation.
Jaworski, Z., Zakrzewska, B., Pianko-Oprych, P., 2017. On thermodynamic equilibrium of carbon deposition from gaseous C-H-O mixtures: updating for nanotubes. Rev. Chem. Eng. 33, 217–235. https://doi.org/doi:10.1515/revce-2016-0022
Jünger, C., 2008. Grundlagenuntersuchungen zur Biomassetrocknung und Entwicklung eines Verfahrens zur Niedertemperaturtrocknung von Hackschnitzel (PhD thesis). TU Wien.
Kaltschmitt, M., Hartmann, H., Hofbauer, H., 2016. Energie aus Biomasse, 3rd ed. Springer Vieweg.
Karl, J., 2014. Biomass heat pipe reformer—design and performance of an indirectly heated steam gasifier. Biomass Convers. Biorefinery 4, 1–14. https://doi.org/10.1007/s13399-013-0102-6
Kirnbauer, F., Hofbauer, H., 2013. The mechanism of bed material coating in dual fluidized bed biomass steam gasification plants and its impact on plant optimization. Powder Technol. 245, 94–104. https://doi.org/10.1016/j.powtec.2013.04.022
Klinski, S., 2006. Einspeisung von Biogas in das Erdgasnetz. nachwachsende-rohstoffe.de.
Knudsen, J.N., Jensen, J.N., Vilhelmsen, P.-J., Biede, O., 2009. Experience with $CO_2$ capture from coal flue gas in pilot-scale: Testing of different amine solvents. Energy Procedia 1, 783–790.
Körner, A., 2015. Technology Roadmap  Hydrogen and Fuel Cells IEA Technology Roadmap.
Kraussler, M., 2018. Evaluation of dual fuidized bed biomass gasification plants generating electricity, valuable gases, and district heat (PhD thesis). TU Wien, Vienna.
Kraussler, M., Binder, M., Fail, S., Bosch, K., Hackel, M., Hofbauer, H., 2016. Performance of a water gas shift pilot plant processing product gas from an industrial scale biomass steam gasification plant. Biomass Bioenergy, Biomass & Bioenergy special issue of the 23rd European Biomass Conference and Exhibition held in Vienna, June 2015 89, 50–57. https://doi.org/10.1016/j.biombioe.2015.12.001
Kraussler, M., Binder, M., Hofbauer, H., 2017. Performance of a water gas shift unit processing tar-rich product gas from a commercial biomass steam gasification plant operating at partial load. Int. J. Oil Gas Coal Technol. 14, 32. https://doi.org/10.1504/IJOGCT.2017.10002097
Kraussler, Michael, Binder, M., Hofbauer, H., 2016. 2250-h long term operation of a water gas shift pilot plant processing tar-rich product gas from an industrial scale dual fluidized

bed biomass steam gasification plant. Int. J. Hydrog. Energy 41, 6247–6258. https://doi.org/10.1016/j.ijhydene.2016.02.137
Kuba, M., 2013. Product Gas Cleaning for Biomass Gasificatin with Focus on Catalytic Tar Decomposition and Peration of a Downstream Reformer (Master Thesis). TU Wien, Vienna.
Kuba, M., Havlik, F., Kirnbauer, F., Hofbauer, H., 2016. Influence of bed material coatings on the water-gas-shift reaction and steam reforming of toluene as tar model compound of biomass gasification. Biomass Bioenergy 89, 40–49. https://doi.org/10.1016/j.biombioe.2015.11.029
Kuba, M., Kraft, S., Kirnbauer, F., Maierhans, F., Hofbauer, H., 2018. Influence of controlled handling of solid inorganic materials and design changes on the product gas quality in dual fluid bed gasification of woody biomass. Appl. Energy 210, 230–240. https://doi.org/10.1016/j.apenergy.2017.11.028
Liu, K., Song, C., Subramani, V., 2010. Hydrogen and syngas production and purification technologies. Wiley, Hoboken, New Jersey.
MacDowell, N., Florin, N., Buchard, A., Hallett, J., Galindo, A., Jackson, G., Adjiman, C.S., Williams, C.K., Shah, N., Fennell, P., 2010. An overview of $CO_2$ capture technologies. Energy Environ. Sci. 3, 1645–1669. https://doi.org/10.1039/c004106h
Meerman, J.C., Hamborg, E.S., Keulen, T. van, RamÄ-rez, A., Turkenburg, W.C., Faaij, A.P.C., 2012. Techno-economic assessment of $CO_2$ capture at steam methane reforming facilities using commercially available technology, International Journal of Greenhouse Gas Control. Int. J. Greenh. Gas Control 9, 160–171. https://doi.org/10.1016/j.ijggc.2012.02.018
Miltner, A., 2010. Techno-ökonomische Analyse der regenerativen Produktion von Wasserstoff für den Einsatz in Fahrzeugen (PhD Thesis). TU Wien.
Mueller-Langer, F., Tzimas, E., Kaltschmitt, M., Peteves, S., 2007. Techno-economic assessment of hydrogen production processes for the hydrogen economy for the short and medium term. Int. J. Hydrog. Energy, TMS06: Symposium on Materials in Clean Power Systems 32, 3797–3810. https://doi.org/10.1016/j.ijhydene.2007.05.027
Müller, S., 2013. Hydrogen from biomass for industry - industrial application of hydrogen production based on dual fluid gasification (PhD thesis). TU Wien, Vienna.
Ni, M., Leung, D.Y.C., Leung, M.K.H., Sumathy, K., 2006. An overview of hydrogen production from biomass. Fuel Process. Technol. 87, 461–472. https://doi.org/10.1016/j.fuproc.2005.11.003
Norman Poboß, 2016. Experimentelle Untersuchung der sorptionsunterstützten Reformierung. Universität Stuttgart.
Paris Agreement, 2015.
Persson, T., 2013. Biogas up-grading: a technical review.
Pfeifer, C., Puchner, B., Hofbauer, H., 2009. Comparison of dual fluidized bed steam gasification of biomass with and without selective transport of CO2. Chem. Eng. Sci. 64, 5073–5083. https://doi.org/10.1016/j.ces.2009.08.014
Privalova, E., Rasi, S., Mäki-Arvela, P., Eränen, K., Rintala, J., Murzin, D.Y., Mikkola, J.P., 2013. $CO_2$ capure from biogas: absorbent selection. RSC Adv. 3, 2979. https://doi.org/10.1039/c2ra23013e
Pröll, T., Rauch, R., Aichernig, C., Hofbauer, H., 2007. Fluidized Bed Steam Gasification of Solid Biomass - Performance Characteristics of an 8 MWth Combined Heat and Power Plant. Int. J. Chem. React. Eng. 5. https://doi.org/10.2202/1542-6580.1398
Rapagnà, S., Gallucci, K., Di Marcello, M., Foscolo, P.U., Nacken, M., Heidenreich, S., Matt, M., 2012. First Al2O3 based catalytic filter candles operating in the fluidized bed gasifier freeboard. Fuel 97, 718–724. https://doi.org/10.1016/j.fuel.2012.02.043
Rapagnà, S., Gallucci, K., Di Marcello, M., Matt, M., Nacken, M., Heidenreich, S., Foscolo, P.U., 2010. Gas cleaning, gas conditioning and tar abatement by means of a catalytic filter candle in a biomass fluidized-bed gasifier. Bioresour. Technol. 101, 7123–7130. https://doi.org/10.1016/j.biortech.2010.03.139

Ratnasamy, C., Wagner, J.P., 2009. Water Gas Shift Catalysis. Catal. Rev. 51, 325–440. https://doi.org/10.1080/01614940903048661
Rochelle, G.T., 2009. Amine Scrubbing for CO2 Capture. Science 325, 1652–1654. https://doi.org/10.1126/science.1176731
Romeo, L.M., Bolea, I., Escosa, J.M., 2008. Integration of power plant and amine scrubbing to reduce $CO_2$ capture costs. Appl. Therm. Eng. 28, 1039–1046. https://doi.org/10.1016/j.applthermaleng.2007.06.036
Ryckebosch, E., Drouillon, M., Vervaeren, H., 2011. Techniques for transformation of biogas to biomethane. Biomass Bioenergy 35, 1633–1645. https://doi.org/10.1016/j.biombioe.2011.02.033
Schildhauer, T.J., Biollaz, S.M. (Eds.), 2016. Synthetic natural gas from coal, dry biomass, and power-to-gas applications. Wiley, Hoboken, New Jersey.
Scholz, M., Melin, T., Wessling, M., 2013. Transforming biogas into biomethane using membrane technology. Renew. Sustain. Energy Rev. 17, 199–212. https://doi.org/10.1016/j.rser.2012.08.009
Sircar, S., 2002. Pressure Swing Adsorption. Ind. Eng. Chem. Res. 41, 1389–1392. https://doi.org/10.1021/ie0109758
Solutions, S.G., 2011. For cost-effective, enhanced removal of carbon dioxide ($CO_2$).
Starr, K., Gabarrell, X., Villalba, G., Talens, L., Lombardi, L., 2012. Life cycle assessment of biogas upgrading technologies. Waste Manag. 32, 991–999. https://doi.org/10.1016/j.wasman.2011.12.016
Technology Roadmap - Hydrogen and Fuel Cells, 2015. . IEA - International Energy Agency.
Thrän, D., Billig, E., Persson, T., Svensson, M., Daniel-Gromke, J., Ponitka, J., Seiffert, M., Baldwin, J., Kranzl, L., Schipfer, F., Matzenberger, J., Devriendt, N., Dumont, M., Dahl, J., Bochmann, G., 2014. Biomethane - status and factors affecting market development and trade. IEA Bioenergy Task 40 and Task 37.
Thunman, H., Seemann, M., Berdugo Vilches, T., Maric, J., Pallares, D., Ström, H., Berndes, G., Knutsson, P., Larsson, A., Breitholtz, C., Santos, O., 2018. Advanced biofuel production via gasification - lessons learned from 200 man-years of research activity with Chalmers' research gasifier and the GoBiGas demonstration plant. Energy Sci. Eng. 6, 6–34. https://doi.org/10.1002/ese3.188
Tobiesen, F.A., Svendsen, H.F., Mejdell, T., 2007. Modeling of Blast Furnace $CO_2$ Capture Using Amine Absorbents. Ind. Eng. Chem. Res. 46, 7811–7819. https://doi.org/10.1021/ie061556j
TVT TU Wien, 2012. Biogas to biomethane technology review. Research Division Thermal Process Engineering and Simulation, TU Wien, Vienna.
Twigg, M.V., 1989. Catalyst Handbook. Manson Publishing.
Urban, W., Girod, K., Lohmann, H., 2009. Technologien und Kosten der Biogasaufbereitung und Einspeisung in das Erdgasnetz. Ergebnisse der Markterhebung 2007-2008. Fraunhofer Institut Umwelt-, Sicherheits, Energietechnik UMSICHT.
Van der Drift, A., Van der Meijden, C.., Boerrigter, H., 2005. MILENA gasification technology for high efficient SNG production from biomass, in: In 14th European Biomass Conference & Exhibition. Paris.
Van der Meijden, C.., 2010. Development of the MILENA gasification technology for the production of Bio-SNG. Technische Universiteit Eindhoven.
Van der Meijden, C.., Van der Drift, A., Vreugdenhil, B.., 2008a. Experimental results from the allothermal biomass gasifier Milena. Presented at the In 15th European Biomass Conference & Exhibition, Berlin.
Van der Meijden, C.., Veringa, H.., Van der Drift, A., Vreugdenhil, B.., 2008b. The 800 kWth allothermal biomass gasifier MILENA., in: In 16th European Biomass Conference & Exhibition.
Voss, B., Madsen, J., Bøgild Hansen, J., Andersson, K.J., 2016. Topsøe Tar Reforming in Skive: The Tough Get Going. Catal. Rev. 2016, Vol 29, Issue 5,p.7-14.
Wang, M., Lawal, A., Stephenson, P., Sidders, J., Ramshaw, C., 2011. Post-combustion CO2 capture with chemical absorption: A state-of-the-art review. Chem. Eng. Res. Des.,

Special Issue on Carbon Capture & Storage 89, 1609–1624. https://doi.org/10.1016/j.cherd.2010.11.005
Wilk, V., Hofbauer, H., 2016. Analysis of optimization potential in commercial biomass gasification plants using process simulation. Fuel Process Techn 141, 138–147. https://doi.org/10.1016/j.fuproc.2015.07.035
Yao, J., Kraussler, M., Benedikt, F., Hofbauer, H., 2017. Techno-economic assessment of hydrogen production based on dual fluidized bed biomass steam gasification, biogas steam reforming, and alkaline water electrolysis processes. Energy Convers. Manag. 145, 278–292. https://doi.org/10.1016/j.enconman.2017.04.084
Zech, K., Grasemann, E., Oehmichen, K., Kiendl, I., Schmersahl, R., Rönsch, S., Weindorf, W., Funke, S., Michaelis, J., Wietschel, M., Seiffert, M., Müller-Langer, F., 2013. Hy-NOW Evaluierung der Verfahren und Technologien für die Bereitstellung von Wasserstoff auf Basis von Biomasse. Leipzig.
Zhu, M., Wachs, I.E., 2016. Iron-Based Catalysts for the High-Temperature Water-Gas Shift (HT-WGS) Reaction: A Review. ACS Catal. 6, 722–732. https://doi.org/10.1021/acscatal.5b02594

IEA Bioenergy

## Further Information

IEA Bioenergy Website
www.ieabioenergy.com

Contact us:
www.ieabioenergy.com/contact-us/